Eelbrain: A Python toolkit for time-continuous analysis with temporal response functions

Christian Brodbeck[1*], Proloy Das[2], Marlies Gillis[3], Joshua P. Kulasingham[4], Shohini Bhattasali[5], Phoebe Gaston[1], Philip Resnik[6] & Jonathan Z. Simon[6]

1) University of Connecticut
2) Massachusetts General Hospital, Harvard Medical School
3) Katholieke Universiteit Leuven
4) Linköping University
5) University of Toronto
6) University of Maryland, College Park

* christian.brodbeck@uconn.edu

1 Abstract

Even though human experience unfolds continuously in time, it is not strictly linear; instead, it entails cascading processes building hierarchical cognitive structures. For instance, during speech perception, humans transform a continuously varying acoustic signal into phonemes, words, and meaning, and these levels all have distinct but interdependent temporal structures. Time-lagged regression using *temporal response functions (TRFs)* has recently emerged as a promising tool for disentangling electrophysiological brain responses related to such complex models of perception. Here we introduce the Eelbrain Python toolkit, which makes this kind of analysis easy and accessible. We demonstrate its use, using continuous speech as a sample paradigm, with a freely available EEG dataset of audiobook listening. A companion GitHub repository provides the complete source code for the analysis, from raw data to group level statistics. More generally, we advocate a hypothesis-driven approach in which the experimenter specifies a hierarchy of time-continuous representations that are hypothesized to have contributed to brain responses, and uses those as predictor variables for the electrophysiological signal. This is analogous to a multiple regression problem, but with the addition of a time dimension. TRF analysis decomposes the brain signal into distinct responses associated with the different predictor variables by estimating a multivariate TRF (mTRF), quantifying the influence of each predictor on brain responses as a function of time(-lags). This allows asking two questions about the predictor variables: 1) Is there a significant neural representation corresponding to this predictor variable? And if so, 2) what are the temporal characteristics of the neural response associated with it? Thus, different predictor variables can be systematically combined and evaluated to jointly model neural processing at multiple hierarchical levels. We discuss applications of this approach, including the potential for linking algorithmic/representational theories at different cognitive levels to brain responses through computational models with appropriate linking hypotheses.

2 Introduction

This paper introduces Eelbrain, a Python toolkit that makes it straightforward to express cognitive hypotheses as predictive computational models and evaluate those predictions against electrophysiological brain responses. The toolkit is based on the idea of decomposing brain signals into distinct responses associated with different predictor variables by estimating a multivariate temporal response function (mTRF), which maps those predictors to brain responses elicited by time-continuous stimulation (Theunissen et al., 2001; Lalor et al., 2006; David et al., 2007). This form of analysis has yielded valuable insights into the way that perception and cognitive processes unfold over time (e.g. Ding and Simon, 2012; Broderick et al., 2018; Brodbeck et al., 2018a; Daube et al., 2019; Di Liberto et al., 2020; Sohoglu and Davis, 2020).

2.1 How to read this Paper

Time-lagged regression using TRFs is a mathematical method for analyzing the stimulus-response relationship between two signals that are evolving as a function of time, i.e., time series, like speech and brain activity measurements. The goal of this paper is to introduce several categories of cognitive neuroscience questions that can be asked using TRFs, and provide recipes for answering them. As such, the paper is not necessarily meant to be read in a linear fashion. The Introduction provides a general motivation for the approach and explains the underlying concepts in an accessible way. The Methods section explains the technical details and implementation in Eelbrain. The Results section demonstrates how the technique can be applied to answer specific questions. The Discussion section highlights some more advanced considerations and caveats that should be kept in mind. The accompanying GitHub repository (https://github.com/Eelbrain/Alice) provides the source code for everything discussed in the paper (README.md contains instructions on how to get started). In addition, the Examples section on the Eelbrain website provides many source code examples for several other basic tasks.

Depending on the background of the reader, these resources can be approached differently – for example, we recommend reading the Introduction and Results sections first to get an idea of the questions that can be answered, and then referring to the Methods for more detailed background information.

2.2 The convolution model for brain responses

The mTRF approach is built on the assumption that the brain response is continuously evolving in time as a function of the recently encountered stimulus (Lalor et al., 2006). Brain responses do not directly mirror a physical stimulus, but rather reflect a variety of transformations of that stimulus. For example, while speech is transmitted through air pressure variations in the kHz range, this signal is transformed by the auditory periphery, and macroscopic cortical responses are better described as responses to the slowly varying envelope of the original broadband signal. Thus, instead of directly predicting brain responses from the stimulus, the experimenter

commonly selects one or several appropriate predictor variables to *represent* the stimulus, for example the low frequency speech envelope (Lalor and Foxe, 2010).

The convolution model is a formal specification of how the stimulus, as characterized by the predictor variables, leads to the response. The stimulus-response relationship is modeled as a linear convolution in time, as illustrated in Figure 1. In contrast to classical analysis approaches that require averaging, the convolution model applies to single trial data and does not require any repetition of identical stimuli. A convolution kernel, or impulse response, characterizes the influence of each elementary unit in a predictor on the response. This kernel is also called the temporal response function (TRF), to distinguish it from the measured response to the stimulus as a whole. In addition to modeling an individual predictor variable (Figure 1-B,C), the convolution model can also incorporate multiple predictor variables through the assumption that responses are additive (Figure 1-D). Each predictor variable is associated with its own TRF, and thus predicts a separable response component. The ultimate response is the sum of those response components at each time point. This additive model is consistent with the fact that macroscopic measurements of electrical brain signals reflect an additive superposition of signals from different brain regions, potentially reflecting separable neural processing (Nunez and Srinivasan, 2006). When multiple predictor variables are jointly predicting a response, the collection of their TRFs is called a multivariate TRF (mTRF). As such, predictor variables can be thought of as hypotheses about how stimuli are represented by the brain, and multiple concurrent predictors can embody distinct hypotheses about how the stimulus is transformed across different brain regions (Brodbeck and Simon, 2020). The additive nature of the convolution model allows it to be applied to comparatively natural stimulus conditions, such as audiobook listening (Hamilton and Huth, 2020; Alday, 2019), while modeling natural variability through different predictor variables rather than minimizing it through experimental design.

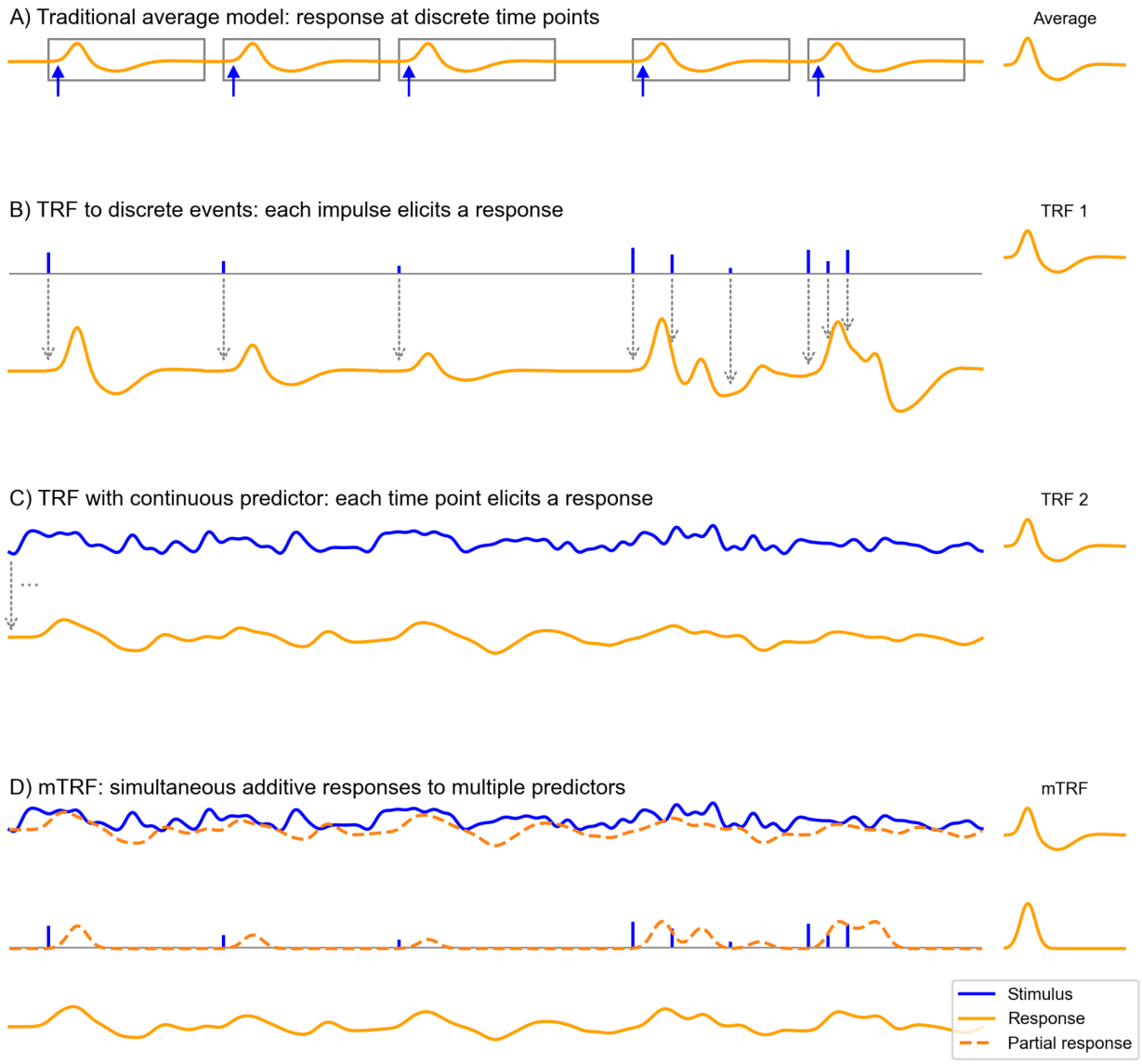
A) Traditional average model: response at discrete time points
Average
B) TRF to discrete events: each impulse elicits a response
TRF 1
C) TRF with continuous predictor: each time point elicits a response
TRF 2
D) mTRF: simultaneous additive responses to multiple predictors
mTRF
Stimulus
Response
Partial response

Figure 1. The convolution model for brain responses as a generalization of the averaging-based paradigm.
(**A**) The traditional event-related analysis method assumes that each stimulus (blue arrows) evokes an identical, discrete response, and this response can be recovered by averaging. This model assumes that responses are clearly separated in time. (**B**) In contrast, the convolution model assumes that each time point in the stimulus could potentially evoke a response. This is implemented with time series predictor variables, illustrated here with a time series containing several impulses. These impulses represent discrete events in the stimulus that are associated with a response, for example the occurrence of words. This predictor time series is convolved with some kernel characterizing the general shape of responses to this event type – the *temporal response function* (TRF), depicted on the right. Gray arrows illustrate the convolution, with each impulse producing a TRF-shaped contribution to the response. As can be seen, the size of the impulse determines the magnitude of the contribution to the response. This allows testing hypotheses about stimulus events that systematically differ in the magnitude of the responses they elicit, for example, that responses increase in magnitude the more surprising a word is. A major advantage over the traditional averaging model is also that responses can be overlapping in time. (**C**) Rather than discrete impulses, the predictor variable in this example is a continuously varying time series. Such continuously varying predictor variables can represent dynamic properties of sensory input, for example the acoustic envelope of the speech signal. The response is dependent on the stimulus in the same manner as in (B), but now every time point of the stimulus evokes its own response shaped like the TRF and scaled by the magnitude of the predictor. Responses are therefore heavily overlapping. (**D**) The multivariate TRF (mTRF) model is a generalization of the TRF model with multiple predictors: like in a multiple regression model, each time series predictor variable is convolved with its own corresponding TRF, resulting in multiple partial responses. These partial responses are summed to generate the actual complete response. Source code: figures/Convolution.py

In most practical data analysis scenarios, the true TRFs are unknown, but the stimulus and the brain responses are known. A TRF estimation algorithm addresses this, by estimating the mTRF that is optimal to predict the brain response from the predictor variables representing the stimulus. Figure 2 illustrates this with EEG responses being predicted from the speech envelope. Typically, this is a very high-dimensional problem – including several predictor variables, each of which can influence the brain response at a range of latencies. Due to the large number of parameters, mTRFs are prone to overfitting, meaning that the mTRFs learn properties of the noise in the specific dataset rather than the underlying, generalizable responses. TRF estimation methods deal with this problem by employing different regularization schemes, i.e., by bringing additional assumptions to the problem that are designed to limit overfitting (see Sparsity prior below). A further step to avoid spurious results due to overfitting is evaluating model quality with cross-validation, i.e., evaluating the model on data that was never used during training. This step allows evaluating whether the mTRF model can generalize to *unseen* data and *predict* novel responses, as opposed to merely *explaining* the responses it was trained on.

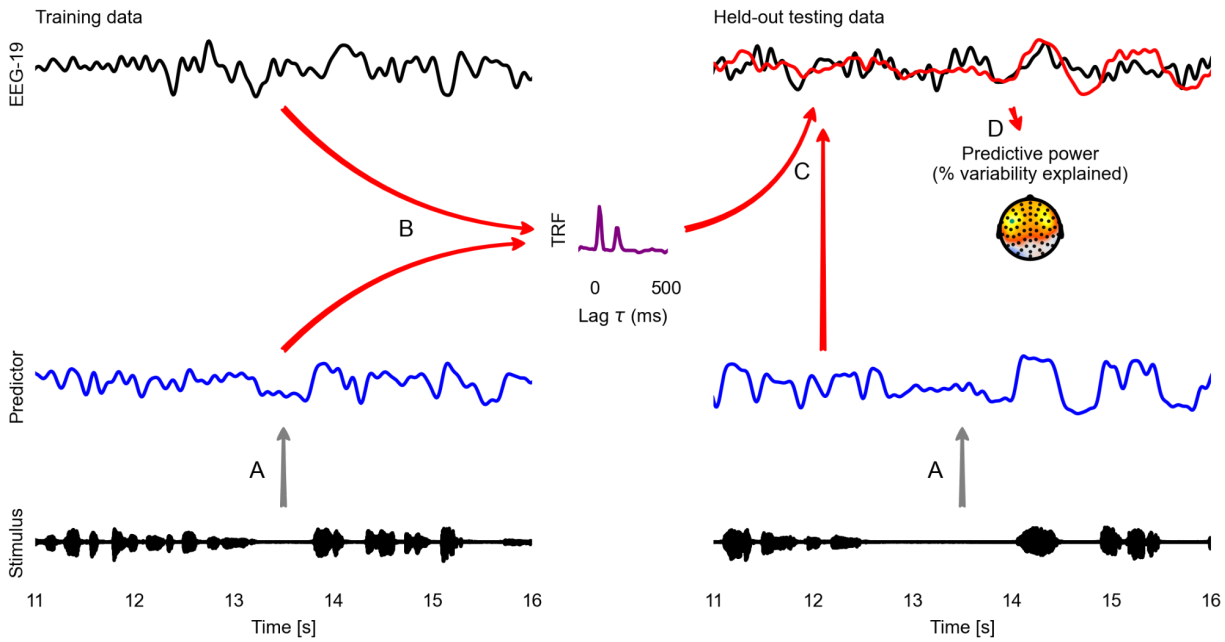

Figure 2. Temporal response function (TRF) analysis of EEG speech tracking.
The left half illustrates the estimation of a TRF model, the right half the evaluation of this model with cross-validation. First, the stimulus is used to generate a predictor variable, here the acoustic envelope (**A**). The predictor and corresponding EEG data (here only one sensor is shown) are then used to estimate a TRF (**B**). This TRF is then convolved with the predictor for the held-out testing data to predict the neural response to the testing data (**C**; measured: black; predicted: red). This predicted response is compared with the actual, measured EEG response to evaluate the predictive power of the model (**D**). A topographic map shows the % of the variability in the EEG response that is explained by the TRF model, estimated independently at each sensor. This head-map illustrates how the predictive power of a predictor differs across the scalp, depending on which neural sources a specific site is sensitive to. The sensor whose data and TRF are shown is marked in green.
Source code: figures/TRF.py.

2.3 Nonlinear responses

Convolution can only model linear responses to a given input, whereas true neural responses are known to be nonlinear. Indeed, nonlinear transformations of the stimulus are arguably the most interesting, because they can show how the brain transforms and abstracts away from the stimulus, rather than merely mirroring it. We advocate a model-driven approach to study such nonlinear responses. A non-linear response can be modeled by generating a predictor variable that applies a non-linear transformation to the original stimulus, and then predicting brain responses as a linear response to this new predictor variable. For instance, it is known that the auditory cortex is disproportionately sensitive to acoustic onsets. This sensitivity has been described with a neural model of auditory edge detection, implemented as a signal processing routine (Fishbach et al., 2001). When this edge detection model is applied to the acoustic

spectrogram, this results in a spectrogram of acoustic onsets, effectively mapping regions in the signal to which specific neuron populations should respond. This transformed spectrogram as a predictor variable thus operationalizes the hypothesis that neurons perform this non-linear transformation. Indeed, such acoustic onset spectrograms are highly significant predictors of auditory magnetoencephalography (MEG) responses (Daube et al., 2019; Brodbeck et al., 2020). Because mTRF models can only use linear transformations of the predictor variables to predict brain responses, a significant contribution from this predictor variable suggests that this non-linear transformation captures the nature of the neural processes giving rise to the brain responses.

This logic for studying nonlinear responses is taken to an even further level of abstraction when language models are used to predict brain responses. For instance, linguistic theory suggests that during speech comprehension, the continuous acoustic signal is transformed into discrete representations such as phonemes and words. However, we do not yet have an explicit, computational model of this transformation that could be used to generate an appropriate predictor. Instead, experimenters can estimate the result of an implicitly specified transformation based on extraneous knowledge, such as linguistic labels and corpus data. For example, responses to phonemes or phonetic features have been modeled through predictors reflecting discrete categories (Di Liberto et al., 2015). Furthermore, a series of such investigations suggests that brain responses to speech reflect linguistic representations at different hierarchical levels (Brodbeck et al., 2018a; Broderick et al., 2018; Weissbart et al., 2020; Gillis et al., 2021; Brodbeck et al., 2022). Such linguistic properties are commonly modeled as impulses corresponding to the onsets of words or phonemes. This does not necessarily entail the hypothesis that responses occur *at word onsets*. Rather, since the mTRFs allow responses at various latencies relative to the stimulus, such predictor variables can predict any time-locked responses that occur in an approximately fixed temporal relationship with the stimulus (within the pre-specified latency window).

During all this, it is important to keep in mind that even predictor variables that implement highly non-linear transformations are still likely to be correlated with the original stimulus (or linear transformations of it). For example, words and phonemes are associated with specific spectro-temporal acoustic patterns which systematically relate to their linguistic significance. Before drawing conclusions about non-linear transformations implemented by the brain, it is thus always important to control for more basic stimulus representations. In the domain of speech processing this includes at least an acoustic spectrogram and an acoustic onsets spectrogram (see Figure 3 below). The latter in particular has been found to account for many responses that might otherwise be attributed to phonetic feature representations (Daube et al., 2019).

2.4 This Tutorial

For this tutorial, we use the openly available Alice dataset (Bhattasali et al., 2020) which contains EEG data from 33 participants who listened to the first chapter of *Alice in Wonderland* (12.4 minutes; 2,129 words). The dataset also includes several word-level regressors derived from different syntactic language models, described in more detail in the original publication

(Brennan and Hale, 2019). Here we implement a complete group level analysis for different levels of representation using Eelbrain.

Eelbrain implements mTRF estimation using boosting (David et al., 2007), as well as a variety of statistical tests, and ways to extract results for further analysis with other tools. The overall implementation of Eelbrain has been guided by the goal of facilitating mTRF estimation, group level analysis, and visualization of results, for a general audience. The choice of boosting is significant as it encourages TRFs with a small number of non-zero coefficients, i.e., the boosting algorithm prefers a simpler explanation over a complex one (Kulasingham and Simon, 2022). This makes boosting suitable for estimating mTRFs for models consisting of structured, highly correlated, and possibly redundant predictor variables (David and Shamma, 2013), as is typical for models in cognitive neuroscience problems.

3 Methods

This section describes each step towards a group level analysis, starting from the data that is included in the open Alice EEG dataset (Bhattasali et al., 2020): EEG recordings, stimulus Wave (audio) files and a comma-separated values (CSV) table with information about the words contained in the audiobook stimuli.

3.1 Overall architecture of the Eelbrain toolbox

Eelbrain provides high level functionality to represent time series data (such as EEG) and functions to work with this data. The `Dataset` class provides a data-table in which each row represents a measurement *case* (e.g., a trial), similar to a dataframe in R. The `Var` and `Factor` classes represent continuous and categorical columns in such a `Dataset`. In addition, the `NDVar` class ("n-dimensional variable") provides a container for n-dimensional data. An `NDVar` instance also carries meta-information, for example sampling rate in a time series, and sensor locations in EEG data. This allows other functions to access that information without user intervention. For example, a plotting function can directly generate topographic plots of an `NDVar` representing event related potential data, without the user specifying which data point corresponds to which sensor, which dimension corresponds to the time axis, what the sampling rate is, etc. More detailed introductions can be found in the Examples section of the Eelbrain online documentation.

3.2 Time series data

In the mTRF paradigm, a time series (for example, voltage at an EEG channel) is modeled as a linear function of one or several other time series (for example, the acoustic envelope of speech). The first step for an mTRF model is thus bringing different time-dependent variables into a common representational format. This is illustrated in Figure 3, which shows an excerpt from the first stimulus in the Alice dataset aligned to the EEG data from the first subject, along with different representations of the stimulus, which can model different neural representations.

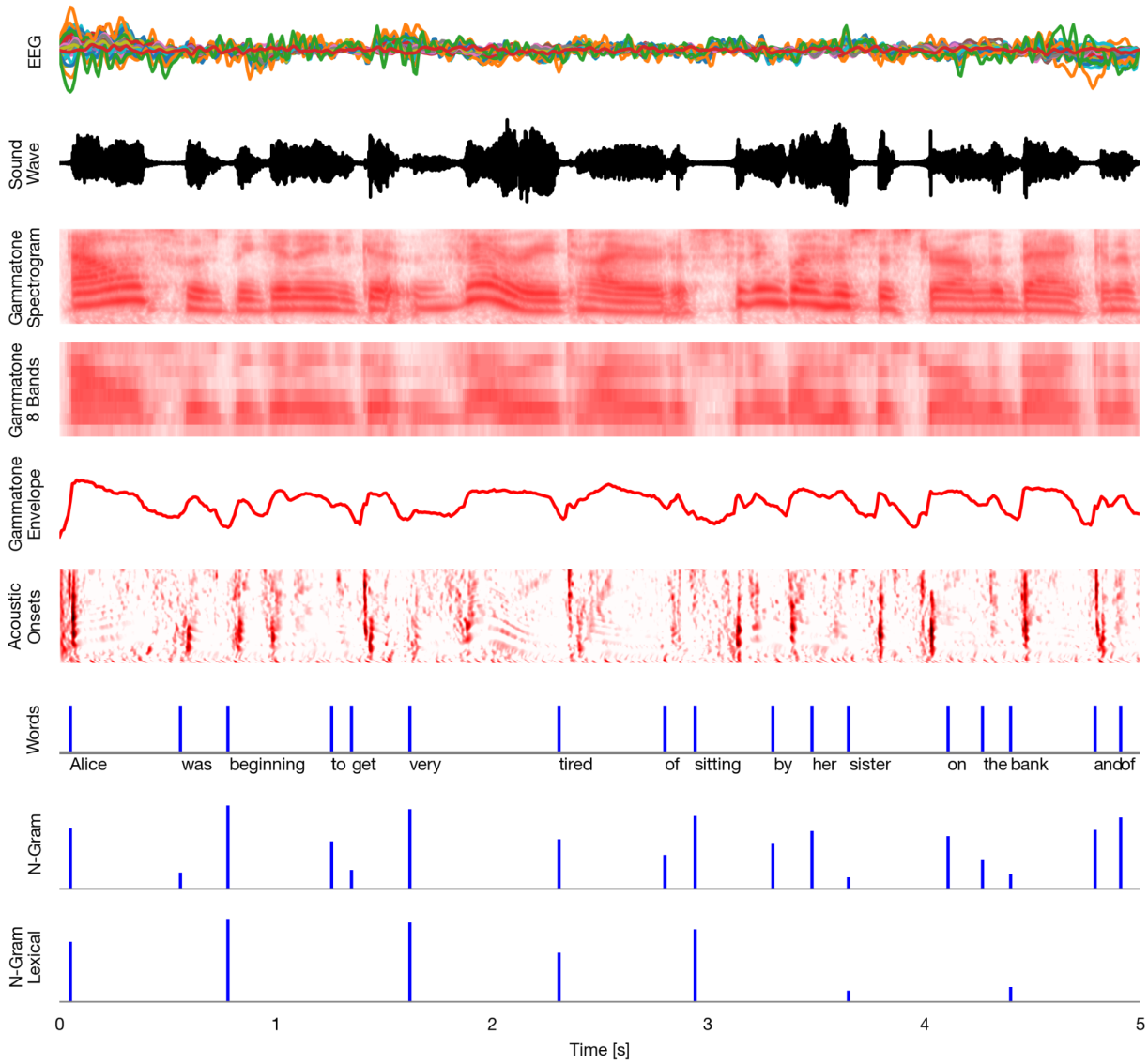
EEG
Sound Wave
Gammatone Spectrogram
Gammatone 8 Bands
Gammatone Envelope
Acoustic Onsets
Words
Alice
was
beginning
to get
very
tired
of
sitting
by
her
sister
on
the bank
and of
N-Gram
N-Gram Lexical
0
1
2
3
4
5
Time [s]

Figure 3. Time series representations of different commonly used speech representations, aligned with the EEG data.
EEG: band-pass filtered EEG responses. Sound Wave: acoustic wave form, time-aligned to the EEG data. Gammatone Spectrogram: spectrogram representation modeling processing at the auditory periphery. Gammatone 8 Bands: the gammatone spectrogram binned into 8 equal-width frequency bins for computational efficiency. Gammatone Envelope: sum of gammatone spectrogram across all frequency bands, reflecting the broadband acoustic envelope. Acoustic Onsets: acoustic onset spectrogram, a transformation of the gammatone spectrogram using a neurally inspired model of auditory edge detection. Words: Uniform impulse predictor at all word onsets, predicting a constant response to all words. N-Gram: Impulses at word onset, scaled with word-level surprisal, estimated from an *n*-gram language model. This predictor will predict brain responses to words that scale with how surprising each word is in its context. N-Gram Lexical: N-Gram surprisal only at content words, predicting a response that scales with surprisal and occurs at content words only.
Source code: figures/Time-series.py

As Figure 3 suggests, time series will often have different dimensions. For example, EEG data might be 2-dimensional with a time and a sensor dimension; a predictor might be one-dimensional, such as the acoustic envelope, or also have multiple dimensions, such as a spectrogram with time and frequency dimensions. To simplify working with different arbitrary dimensions, Eelbrain uses the `NDVar` (*n*-dimensional variable) class. An `NDVar` instance associates an n-dimensional numpy array (Harris et al., 2020) with *n* dimension descriptors. For example, the EEG measurements can be represented by a 2-dimensional `NDVar` with two dimensions characterizing the EEG sensor layout (`Sensor`) and the time axis, as a uniform time series (`UTS`).

The first step for the mTRF analysis is thus to import the EEG measurements and predictor variables as `NDVar` objects, and align them on the time axis, i.e., make sure they are described by identical `UTS` dimensions. The `eelbrain.load` module provides functions for importing different formats directly, such as MNE-Python objects and Wave files (`NDVar` objects can also be constructed directly from `numpy` arrays). Keeping information about dimensions on the `NDVar` objects allows for concise and readable code for tasks such as aligning, plotting, etc. The code for Figure 2 includes an example of loading a Wave file and aligning its time axis to the EEG data through filtering and resampling.

3.2.1 EEG data

EEG data should be pre-processed according to common standards. In the Python ecosystem, MNE-Python offers a unified interface to a variety of EEG file formats and preprocessing routines (Gramfort et al., 2014). Here, we rely on the preprocessed data provided with the Alice EEG dataset, referenced to the averaged mastoids, and processed for artifact reduction with independent component analysis (see Bhattasali et al., 2020). However, a crucial additional step is filtering and downsampling the EEG data. When analyzing continuous electrophysiological recordings, removing low frequencies (i.e., high-pass filtering) takes the place of baseline correction, by removing high-amplitude slow drifts in the EEG signal which would otherwise

overshadow effects of interest. Removing high frequencies, beyond the signals of interest (low-pass filtering), reduces noise and, more crucially, allows conducting the analysis at a lower sampling rate. This makes the analysis faster, because TRF estimation is computationally demanding, and processing times scale with the sampling rate. The major cortical phase-locked responses decrease quickly above 10 Hz (Ding et al., 2014), although there can be exceptions, such as a pitch-following response up to 100 Hz (Kulasingham et al., 2020). For the purpose of this tutorial we are interested in the range of common cortical responses and apply a 0.5-20 Hz band-pass filter. Theoretically, a sampling rate exceeding 2 times the highest frequency (also known as Nyquist frequency) is necessary for a faithful representation of the signal. However, Nunez and Srinivasan (2006) recommend a sampling rate 2.5 times the highest frequency due to various empirical considerations, such as presence of random jitters, finite roll-off of the band-pass filter, etc. An even higher rate could be desirable for some secondary analysis and visualization, since it leads to smoother results. Here we conduct the analysis with a sampling rate of 100 Hz.

EEG data usually contain markers that indicate the start of the stimulus presentation. These can be used to quickly extract EEG data time-locked to the stimuli in the required time series format, i.e. a 2-dimensional `NDVar` with `Sensor` and `UTS` dimensions (see source code to Figure 2).

3.2.2 Predictor variables

Any hypothesis about time-locked neural processing that can be quantified can be represented by a time series derived from the stimulus. Here we will illustrate two approaches: The first approach implements hypotheses about spectro-temporal transformations of the acoustic signal by directly applying those transformations to the speech waveform. The second approach implements hypotheses about linguistic processing based on experimenter-determined, discrete linguistic events.

3.2.2.1 Time-continuous predictor variables: gammatone spectrogram and derivatives

A common starting point for modeling acoustic responses is through a model of the cochlear transformation of the sound. Here we use the gammatone spectrogram method to estimate cochlear transformations (Patterson et al., 1992; Heeris, 2018). A gammatone spectrogram is initially a high-dimensional representation, with more than a hundred time series representing the acoustic power at different frequency bands. For computational efficacy, we reduce the number of bands by summarizing several contiguous bands into one. Here we use 8 bands as a compromise that leaves the global acoustic structure intact (Figure 3). An extreme form of this dimension reduction is using the acoustic envelope, which summarizes the entire spectrogram with a single band.

In addition to representing raw acoustic features, the auditory cortex is known to prominently represent acoustic onsets (Daube et al., 2019). Here we model such representations by applying the neurally inspired auditory edge detection transformation to the gammatone spectrogram (Brodbeck et al., 2020). It is also common to approximate such a transformation through the half-wave rectified derivative of the acoustic envelope (Fiedler et al., 2017; Daube et al., 2019).

Because these predictor variables will be used repeatedly, it is convenient to generate them once and save them for future use. The script `predictors/make_gammatone.py` loops through all stimuli, computes a high-dimensional gammatone spectrogram (a 2-dimensional `NDVar` with `frequency` and `UTS` dimensions), and saves it as a Python pickle file via the `eelbrain.save` module. The script `predictors/make_gammatone_predictors.py` loads these high-dimensional spectrograms via the `eelbrain.load` module and resamples them to serve as predictors, and it also applies the onset transformation and saves the resulting predictors.

Eelbrain provides functions to quickly generate this auditory model from audio files (`gammatone_bank` and `edge_detector`), as well as some basic signal processing routines for `NDVar`s (e.g., `filter_data`; see the Reference section of the online documentation for a list). Different models can be constructed using different tools and converted to `NDVar`s (for an example of importing data from a `*.mat` file, see the *EEG speech envelope TRF* example of the online documentation).

3.2.2.2 Discrete predictor variables

The analysis of linguistic representations, which cannot be derived directly from the sound waveform, commonly relies on forced alignment, a method that infers time-stamps for phoneme and word boundaries by comparing the sound waveform with a transcript. An example of an open source forced aligner with extensive documentation is the Montreal Forced Aligner (e.g. McAuliffe et al., 2017). Because the forced alignment procedure requires some additional steps that are well documented by the respective aligners we skip it here, and instead use the word-onset time-stamps provided with the Alice dataset.

Discrete predictors come in two varieties: constant magnitude impulses and variable magnitude impulses (see Figure 3, lower half). Constant magnitude impulses always have the same magnitude, for example an impulse of magnitude 1 at each word onset. Such a predictor implements the hypothesis that all words are associated with a shared characteristic brain response, similar to an event-related potential (ERP). The TRF estimation algorithm will then determine the latencies relative to those impulses at which the brain exhibits a consistent response. Variable magnitude impulses implement the hypothesis that the brain response to each word varies systematically with some quantity. For example, the N400 is assumed to co-vary with how surprising the word is in its context. A predictor with an impulse at each word onset, whose magnitude is equal to the surprisal of that word, will enable predicting a stereotyped response to words whose amplitude linearly varies with word surprisal. The linking hypothesis here is that for each event, the brain responds with population activity that scales in amplitude with how surprising that event is, or how much new information it provides (see e.g. Brodbeck et al., 2022).

The Alice dataset comes with a table including all time-stamps and several linguistic properties (`stimuli/AliceChapterOne-EEG.csv`). Each row of this table represents one word, and contains the time point at which the word starts in the audio file, as well the surprisal values that were used to relate the EEG signal to several language models in the original analysis (Brennan and Hale, 2019). Such a table listing event times and corresponding feature values is

sufficient for constructing appropriate regressors on the fly, and has a much lower memory footprint than a complete time series. The script `predictors/make_word_predictors.py` converts the table into the Eelbrain `Dataset` format that can be directly used to construct the regressor as an `NDVar`. To keep a common file structure scheme with the continuous regressors, such a table is generated for each stimulus.

Eelbrain provides a function for turning any time/value combination, reflecting the occurrence of discrete events, into a continuous predictor variable: `event_impulse_predictor`. The time/value pairs can either be constructed directly in Python, or can be imported, for example from a text file using the `load.tsv` function.

3.3 TRF estimation

3.3.1 Background: The convolution model

The key assumption behind the mTRF approach is that the dependent variable, y, is the result of a convolution (linear filtering) of one or several predictor variables, x, with a corresponding filter kernel h. For a single predictor variable, the model is formulated as the convolution of the predictor variable with a one-dimensional filter kernel. For example, y_t might be the value of an EEG channel at time t, and x_t the value of the acoustic envelope at time t:

$$y_t = \sum_{\tau=\tau_{min}}^{\tau_{max}} h_\tau x_{t-\tau}$$

Here h represents the filter kernel, also known as TRF, and τ enumerates the time delays or lags between y and x at which x can influence y. To extend this approach to multiple predictor variables, it is assumed that the individual filter responses are additive. In that case, x consists of n predictor time series and thus has two dimensions, one being the time axis and the other reflecting n different predictor variables. The corresponding multivariate TRF (mTRF) is also two-dimensional, consisting of one TRF for each predictor variable:

$$y_t = \sum_{i=0}^{n} \sum_{\tau=\tau_{min}}^{\tau_{max}} h_{i,\tau} x_{i,t-\tau}$$

This model allows predicting a dependent variable y, given predictors x and mTRF h.

In neural data analysis scenarios, typically the measured brain response and the stimuli are known, whereas the filter kernel h is unknown. This leads to two reformulations of the general problem in which x and y are known, and h is to be estimated; these represent alternative approaches for analysis. In the first, the so-called forward or encoding model, h is optimized to predict brain responses from stimulus representations. In the second, the so-called backward, or decoding model, h is optimized to reconstruct a stimulus representation from the neural measurements. The problems can both be expressed in the same general form and solved with the same algorithms. Eelbrain provides an implementation of the boosting algorithm (David et al., 2007), further described in Background: Boosting implementation below.

3.3.2 Forward model (encoding)

Given a continuous measurement and one or more temporally aligned predictor variables, the reverse correlation problem consists of finding the filter kernel, or mTRF, that optimally predicts the response from the stimuli. The result of the convolution now becomes the predicted response:

$$\hat{y}_t = \sum_{i=0}^{n} \sum_{\tau=\tau_{min}}^{\tau_{max}} h_{i,\tau} x_{i,t-\tau} \tag{1}$$

The goal of the algorithm estimating the mTRF h is to minimize the difference between the measured response y_t and the predicted response $\hat{y}_t$. Figure 2 illustrates estimation of a forward model for EEG data.

The `eelbrain.boosting` function provides a high-level interface for estimating mTRFs and returns a `BoostingResult` object with different attributes containing the mTRF and several model fit metrics for further analysis. Usually, for a forward model, the brain response is predicted from the predictors using positive (i.e. causal) lags. For example,

```
trf = boosting(eeg, envelope, 0, 0.500)
```

would estimate a TRF to predict EEG data from the acoustic envelope, with stimulus lags ranging from 0 to 500 ms (Eelbrain uses seconds as the default time unit). This means that an event at a specific time in the acoustic envelope could influence the EEG response in a window between 0 and 500 ms later. If the dependent variable has multiple measurements, for example as here multiple EEG channels, Eelbrain automatically assumes a mass-univariate approach and estimates a TRF for each channel. Negative lags, as in

```
trf = boosting(eeg, envelope, -0.100, 0.500)
```

are non-causal in the sense that they assume a brain response that precedes the stimulus event. Such estimates can nevertheless be useful for at least two reasons. First, if the stimulus genuinely represents information in time, then non-causal lags can be used as an estimate of the noise floor. As such they are analogous to the baseline in ERP analyses, i.e., they indicate how variable TRFs are at time points at which no true response is expected. Second, when predictor variables are experimenter-determined, the temporal precision of the predictor time series might often be reduced, and information in the acoustic speech signal might in fact precede the predictor variable. In such cases, the negative lags might be diagnostic. For example, force-aligned word and phoneme onsets assume the existence of strict boundaries in the speech signal, when in fact the speech signal can be highly predictive of future phonemes due to coarticulation (e.g. Salverda et al., 2003).

An advantage of the forward model is that it can combine information from multiple predictor variables. The boosting algorithm in particular is robust with a large number of (possibly correlated) predictor variables (e.g., David and Shamma, 2013). Eelbrain supports two ways to specify multiple predictor variables. The first is using a multi-dimensional predictor, for example

a two-dimensional NDVar, spectrogram with frequency and UTS dimensions. These are used with the boosting function just like one-dimensional time series, and will be treated as multi-dimensional predictor variables, i.e., the different frequency bands will be jointly used for the optimal prediction of the dependent variable:

```
mtrf = boosting(eeg, spectrogram, 0, 0.500)
```

The second option for using multiple predictor variables is specifying them as a list of NDVar (one and/or two-dimensional), for example:

```
mtrf = boosting(eeg, [envelope, spectrogram], 0, 0.500)
```

3.3.3 Backward model (decoding)

Instead of predicting the EEG measurement from the stimulus, the same algorithm can attempt to reconstruct the stimulus from the EEG response. The filter kernel is then also called a decoder. This can be expressed with (1), but now y_t refers to a stimulus variable, for example the speech envelope, and $x_{i,t}$ refers to the EEG measurement at sensor i and time t. Accordingly, a backward model can be estimated with the same boosting function. For example,

```
decoder = boosting(envelope, eeg, -0.500, 0)
```

estimates a decoder model to reconstruct the envelope from the EEG data. Note the specification of delay values τ in the boosting function, from the point of view of the predictor variable: because each point in the EEG response reflects the stimulus preceding it, the delay values are negative, i.e., a given point in the EEG response should be used to reconstruct the envelope in the 500 ms window preceding the EEG response.

Because the EEG channels now function as the multivariate predictor variable, all EEG channels are used jointly to reconstruct the envelope. An advantage of the backward model is that it thus combines data from all EEG sensors to reconstruct a stimulus feature. It provides a powerful measure of how much information about the stimulus is contained in the brain responses, taken as a whole. A downside is that it does not provide a straight-forward way for distinguishing responses that are due to several, correlated predictor variables. For this reason, we will not further discuss it here. However, backward models have applications in other domains, where questions are not about specific representations, for instance attention decoding in auditory scenes (O'Sullivan et al., 2015).

3.4 Background: The boosting algorithm

The general TRF estimation problem, i.e., finding the optimal filter kernels in forward and backward models, can be solved with different approaches. The Eelbrain toolkit implements the boosting algorithm, which is resilient to over-fitting and performs well with correlated predictor variables (David et al., 2007; David and Shamma, 2013). The boosting algorithm is intentionally designed with a bias to produce sparse mTRFs, i.e., mTRFs in which many elements are exactly

zero. The algorithm thus incorporates a so-called sparsity prior, i.e., a prior to favor sparser models over alternatives (see Section 5.2 Sparsity prior).

Boosting starts by dividing the data into training and validation folds, and initializing an empty mTRF (all values $h_{i,\tau}$ are initially set to 0). It then iteratively uses the training data to find the element in the filter kernel which, when changed by a fixed small amount `delta`, leads to the largest error reduction. Figure 4 shows pseudo-code for the boosting algorithm. For multiple predictors, the search is performed over all the predictors as well as time lags, essentially letting the different predictors compete to explain the dependent variable. At each step, only a single element in the mTRF is modified. In that respect, boosting is a coordinate descent algorithm because it moves only at right angles in the parameter space. This promotes sparsity, as most elements stay at zero in every step. After each such `delta` change, the validation data is consulted to verify that the error is also reduced in the validation data. Once the error starts increasing in the validation set, the training stops. This early stopping strategy prevents the model from overfitting to the training data. In other words, the early stopping strategy in the boosting algorithm acts as an implicit prior to promote sparsity, i.e., it forces unimportant filter kernel coefficients to remain exactly 0.

```
mTRF[:] = 0
n_validation_error_increased = 0

while n_validation_error_increased < 2:
  current_training_error = error of mTRF in training set
  current_validation_error = error of mTRF in validation set

  # Find training error for all possible coordinate steps
  for element in mTRF:
    error_add[element] = error of mTRF with element = element + Δ
    error_sub[element] = error of mTRF with element = element - Δ

  # If no error reduction is possible, reduce Δ or stop
  if smallest error in error_add, error_sub > current_training_error:
    Δ *= 0.5
    if Δ ≥ mindelta:
      continue
    else:
      break

  # Update the mTRF and check validation set error
  mTRF = mTRF corresponding to smallest error in error_add, error_sub
  new_validation_error = error of mTRF in validation set
  if new_validation_error > current_validation_error:
    n_validation_error_increased += 1
  else:
    n_validation_error_increased = 0

mTRF = the mTRF in the history with the smallest validation error
```

Figure 4. Pseudo-code for the default version of the boosting algorithm.

The default implementation of the boosting algorithm constructs the kernel from impulses (each element $h_{i,\tau}$ is modified independently), which can lead to temporally discontinuous TRFs. In order to derive smoother TRFs, TRFs can be constructed from a basis of smooth window functions instead. In Eelbrain, the basis shape and window size are controlled by the `basis` and `basis_window` parameters in the `boosting` function. Their use is described in more detail in section 3.8.

Additionally, when using multiple predictors, it may be undesirable to stop the entire model training when a single predictor starts overfitting. In that case, the `selective_stopping` option allows freezing only the predictor which caused the overfitting, while training of the TRF components corresponding to the remaining predictors continues, until all predictors are frozen.

Finally, the default error metric for evaluating model quality is the widely used ℓ_2 error. Due to squaring, however, the ℓ_2 error is disproportionately sensitive to time points with large errors. Specifically in electrophysiology, large errors are typically produced by artifacts, and it is undesirable to give such artifacts a large influence on the model estimation. Since it is not trivial to exclude time-intervals containing such artifacts from the analysis in continuous data, Eelbrain also allows use of the ℓ_1 error norm through the `error='l1'` argument, which improves robustness against such outlier data.

Usually both the dependent variable and the predictor are centered around zero, and either standardized against the standard deviation (for ℓ_2 error) or normalized by the ℓ_1 norm (for ℓ_1 error) before starting the boosting algorithm. The centering step is crucial to eliminate the intercept, since the boosting algorithm prefers sparse solutions, i.e., solutions with exact zero coefficients. When multiple predictors are used, this preprocessing step is applied separately to each of them, to ensure none of them affects the boosting procedure disproportionately. If required, this preprocessing step can be skipped through an argument to the `boosting` function: `scale_data=False`.

3.4.1 Cross-validation

By default, the `boosting` function trains an mTRF model on all available data. Reserving some data for cross-validation, which further reduces overfitting, can be enabled by setting the `test` parameter to `test=True`. Since the boosting algorithm already divides the data into training and validation sets, enabling cross-validation entails splitting the data into three segments for each run: training, validation, and test sets. While the training and validation segments are consulted for estimating the TRFs (as described above), the test segment does not influence the estimation of the TRFs at all. Only once the TRF estimation is finalized, the final TRF is used to predict the responses in the test segment. To use the data optimally, Eelbrain automatically implements k-fold cross-validation, whereby the data is divided into k partitions, and each partition serves as the test set once (see Data partitions Eelbrain example). Thus, through k-fold cross-validation, the whole response time series can be predicted from unseen data. The

proportion of the explained variability in this response constitutes an unbiased estimate of the predictive power of the given model. The `BoostingResult` object returned by the `boosting` function contains all these metrics as attributes for further analysis.

3.4.2 Comparison to ridge regression

An alternative approach to boosting is ridge regression (Crosse et al., 2021), which uses Tikonov regularization. Tikonov regularization biases the mTRFs to suppress mTRFs in the stimulus subspace with low signal to noise ratio, effectively imposing a smooth prior on the mTRF. In other words, Tikonov regularization tends to distribute the TRF power over all time-lags. In contrast, boosting minimizes nonzero parameters in mTRFs, effectively imposing a sparseness prior on the mTRF, i.e., boosting concentrates the TRF power within a few time-lags. For a detailed discussion on the differences between boosting and ridge regression see David et al. (2007). Figure 5 shows a side by side comparison between boosting and ridge regression in a simulation study where a gammatone spectrogram was used to simulate the time-locked EEG response.

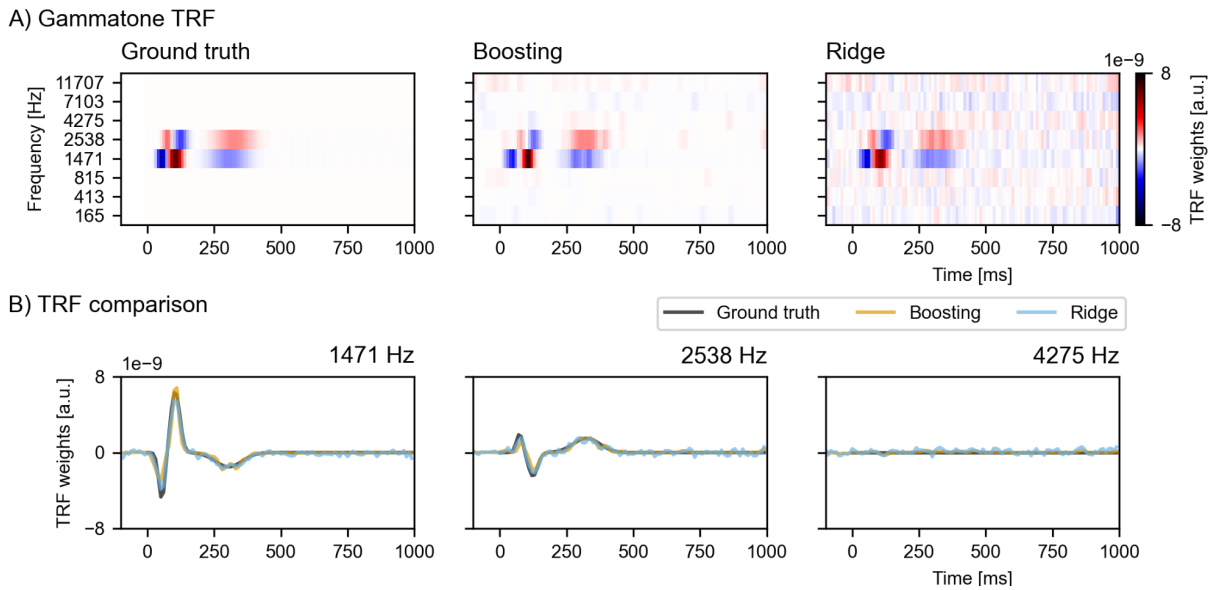

Figure 5. Simulation study comparing boosting with ridge regression when modeling multiple correlated variables.

(**A**) The mTRF used to generate the simulated EEG data (left panel), and mTRFs recovered by boosting and ridge regression (middle and right panel). (**B**) Overlays of boosting, ridge regression and ground truth TRFs at different center frequencies for comparison. Note that the ridge TRF follows the ground truth closely, but produces many false positives. On the contrary, the boosting TRF enjoys an excellent true negative rate, at the expense of biasing TRF peaks and troughs toward 0.

a.u.: arbitrary units. Source code: figures/Collinearity.py.

Briefly, two adjacent gammatone bands (structured, highly correlated variables) were assumed to drive the auditory response with a spatiotemporally alternating pattern (Figure 5-A, left panel). The simulated auditory response was then corrupted with additive pink noise to

simulate EEG activity. We used the `boosting` function from Eelbrain and the ridge regression implementation from the pyEEG toolbox (https://github.com/Hugo-W/pyEEG) to recover the mTRFs from the simulated EEG. For both algorithms, we used 10-fold cross-validation to select the optimum amount of regularization. With boosting we further tuned the `selective_stopping` hyper-parameter according to the explained variances in unseen data (with the `test=True` setting), i.e., we chose the model with the maximal `selective_stopping`, after which the explained variance started decreasing. For boosting, the TRFs are constructed from a basis of hamming windows with window length of 50 ms, resulting in smoother TRFs. Both the mTRFs recovered by boosting and ridge regression capture the dominant features of the ground truth mTRF. However, the boosting mTRF is has only a few peaks and troughs, giving a simpler representation with peaks and troughs closely corresponding to those of the ground truth, while the ridge regression mTRF includes many additional noisy peaks and troughs (Figure 5-A, middle and right panel) (see also David et al., 2007; David and Shamma, 2013). In order to emphasize the differences between the estimates, the mTRF components are shown at the two Gammatone frequency-bands driving the response (Figure 5-B, left and middle panel), and at another frequency-band with no response (rightmost panel). The ridge regression follows the dominant peaks and troughs of the ground truth mTRF closely, but, in doing so, acquires numerous false positives, i.e., small non-zero values when the true mTRF is actually zero. On the other hand, the boosting mTRF displays a high true negative rate, while biasing the peaks and troughs towards zero. The two algorithms are further compared using multiple criteria in Kulasingham and Simon (2022).

3.5 Evaluating predictive power

In practice, a research question can often be operationalized by asking whether a specific predictor variable is neurally represented, i.e., whether it is a significant predictor of brain activity. Different predictor variables of interest are very often correlated in naturalistic stimuli such as speech. It is thus important to test the explanatory power of a given variable while controlling for the effect of other, correlated variables. A powerful method for this is comparing the predictive power of minimally differing sets of predictor variables using cross-validation.

In this context, we use the term ‘model’ to refer to a set of predictor variables, and ‘model comparison’ refers to the practice of comparing the predictive power of two models on held-out data. It is important to re-estimate the mTRFs for each model under investigation to determine the effective predictive power of that model, because mTRFs are sensitive to correlation between predictors and can thus change depending on what other predictors are included during estimation.

When building models for a specific model comparison, we recommend a hierarchical approach: both models should include lower-level properties that the experimenter wants to control for, while the models should differ only in the feature of interest. For example, to investigate whether words are associated with a significant response after controlling for acoustic representations, one could compare the explained variability of (2) and (3):

gammatone spectrogram + onset spectrogram (2)

gammatone spectrogram + onset spectrogram + word onset impulses (3)

If the model in (3) is able to predict held-out test data better than that in (2) then this difference can be attributed to a predictive power of word onset impulses over and above the spectrogram-based representations.

Estimating such mTRF models is the computationally most demanding part of this analysis. For this reason, it usually makes sense to store the result of the individual estimates. The script `analysis/estimate_trfs.py` implements this, by looping through all subjects, fitting mTRFs for multiple models, and saving the results for future analysis.

3.6 Group analysis

In order to statistically answer questions about the predictive power of different models we will need to combine the data from different measurements, usually different subjects. To combine data from multiple subjects along with meta-information such as subject and condition labels Eelbrain provides the `Dataset` class, analogous to data-table representations in other statistics programs such as a dataframe in `R` or `Pandas`, but with the added capability of handling data from `NDVars` with arbitrary dimensionality.

A standard way of constructing a `Dataset` is collecting the individual cases, or rows of the desired data table, and then combining them. The following short script provides a template for assembling a table of model predictive power for several subjects and two models (assuming the mTRF models have been estimated and saved accordingly):

```
cases = []
for subject in ['1', '2', '3']:
    for model in ['sgrams', 'sgrams+words']:
        mtrf = load.unpickle(f"path/to/{subject}_{model}.pickle")
        cases.append([subject, model, mtrf.proportion_explained])
column_names = ['subject', 'model', 'explained']
data = Dataset.from_caselist(column_names, cases)
```

Thus, even though the `proportion_explained` attribute might contain 64 EEG channels (i.e., an `NDVar` with `sensor` dimension) it can be handled as a single entry in this data-table.

3.6.1 Statistical tests

Statistical analysis of mTRFs faces the issue of multiple comparison common in neuroimaging (Maris and Oostenveld, 2007). One way around this is to derive a univariate outcome measure. The (average) predictive power across all sensors is a measure of the overall predictive power of a model. If a prior hypothesis about the location of an effect is available, then the average

predictive power at a pre-specified group of sensors can serve as a more targeted measure, for example:

```
sensors = ['45', '34', '35']
data['explained_average'] = data['explained'].mean(sensor=sensors)
```

Eelbrain implements a limited number of basic univariate statistical tests in the `test` module, but more advanced statistical analysis can be performed after exporting the data into other libraries. All univariate entries in a `Dataset` can be transferred to a `pandas.DataFrame` (Reback et al., 2021) with

```
dataframe = data.as_dataframe()
```

for analysis with other Python libraries like Pingouin (Vallat, 2018), or saved as a text file with

```
data.save_txt('data.txt')
```

to be transferred to another statistics environment like `R` (R Core Team, 2021).

Instead of restricting the analysis to a priori sensor groups, Eelbrain implements several mass-univariate tests (Nichols and Holmes, 2002; Maris and Oostenveld, 2007; Smith and Nichols, 2009). These tests, implemented in the `eelbrain.testnd` module (for n-dimensional tests), are generally based on calculating a univariate statistic at each outcome measure (for example, a t value corresponding to a repeated-measures t-test comparing the predictive power of two models at each EEG sensor), and then using a permutation-based approach for estimating a null distribution for calculating p-values that control for family-wise error. In Eelbrain, these tests can be applied to `NDVars` similarly to univariate tests, with additional arguments for controlling multiple comparison correction. The script to Figure 8 demonstrates a complete group analysis pipeline, from loading pickled mTRF models into a `Dataset` to plotting statistical results.

Mass-univariate tests can provide a detailed characterization of a given comparison, but calculating effect sizes for such results is not straight-forward. For power analyses, carefully selected univariate outcome variables are usually more effective.

3.7 TRF analysis

While predictive power is the primary measure to assess the quality of a model, the TRFs themselves also provide information about the temporal relationship between the brain response and the stimuli. A TRF is an estimate of the brain's response to an impulse stimulus of magnitude 1 (i.e., the impulse response). It thus characterizes the brain response as a function of time relative to stimulus events, analogous to an ERP to a simple stimulus. For example, the TRF estimated to an acoustic envelope representation of speech commonly resembles the ERP to simple tone stimuli. The mTRFs can thus be analyzed in ways that are analogous to ERPs, for example using mass-univariate tests or based on component latencies. Figure 8 demonstrates a representative analysis of TRFs and mTRFs corresponding to different auditory features.

3.8 Meta-parameter: basis function

There are at least two reasons for selecting a basis function as part of the boosting algorithm for TRF estimation. First, constraining the TRFs to neurally more realistic shapes may increase the predictive power of the TRF model. Second, the resulting TRFs are smoother and thus easier to interpret and compare across subjects. Figure 6 illustrates the effect of using a basis function, comparing a 50 or 100 ms wide Hamming window basis with the default impulse basis ("0"). In this case a 50 ms Hamming window basis leads to significantly better predictive power than the default impulse basis (Figure 6-A). TRFs are illustrated using a single sensor which exhibits a strong auditory response (Figure 6-B). Figure 6-C shows that using a wider basis window leads to markedly smoother TRFs, and increases the overlap of the TRFs between two subjects. The basis windows themselves are shown in panel D.

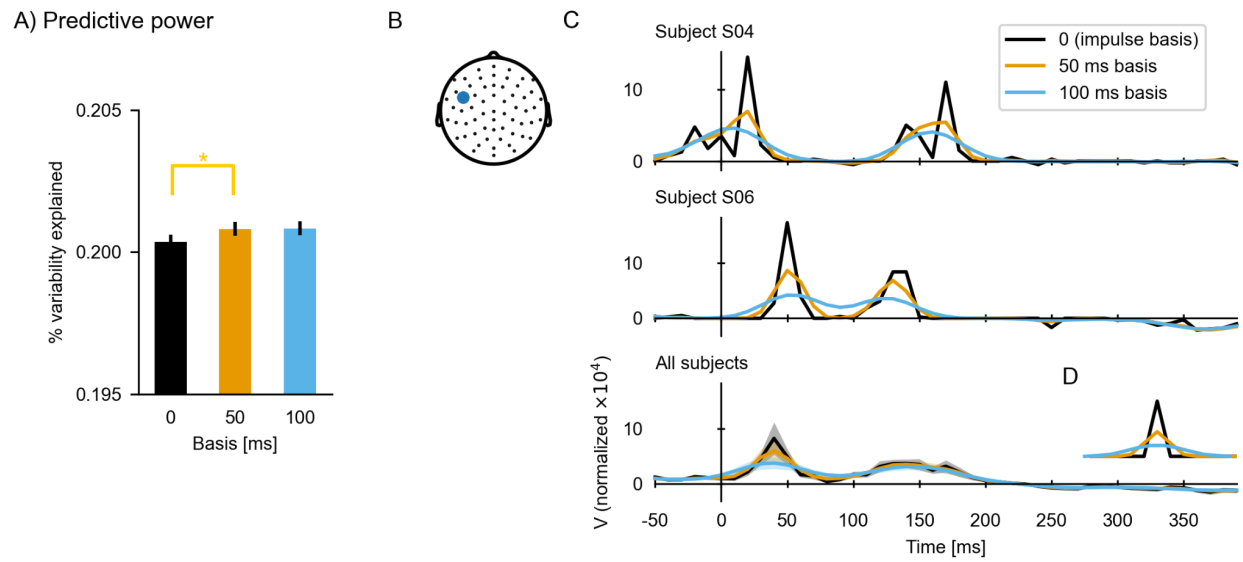

Figure 6. The effect of using a basis function for TRF estimation.
(**A**) Predictive power of the TRFs estimated with different basis windows (expressed as percent of the variability in the EEG data that is explained by the respective TRF model). (**B**) Sensor selected for illustrating TRFs. (**C**) TRFs for a single subject and the average across subjects. (**D**) Basis windows. Notice that the impulse basis ("0") is only a single sample wide, but it appears as a triangle in a line plot with the apparent width determined by the sampling rate.
Source code: figures/TRF-Basis.py

4 Results

A critical goal of mTRF analysis for studying perception is evaluating brain responses that are nonlinear functions of the stimulus. In this section we illustrate this by addressing increasingly complex nonlinear responses.

4.1 Response scale

A basic nonlinearity is that of scale: brain responses can grow nonlinearly with the scale of the input. For instance, in the auditory system, neural responses tend to scale logarithmically with acoustic power encoded in a spectrogram (Rahman et al., 2020). This means that the same amount of power increase in the acoustic signal will cause a different increase in the brain response depending on the initial acoustic power value (see Figure 7-A). Such nonlinear responses are typically modeled by scaling the predictor variable and assuming a linear relationship between the scaled predictor and response (e.g., Fox, 2008). Here we determine the nonlinear relationship between acoustic power and brain response by comparing linear, logarithmic and power law (Biesmans et al., 2017) scales.

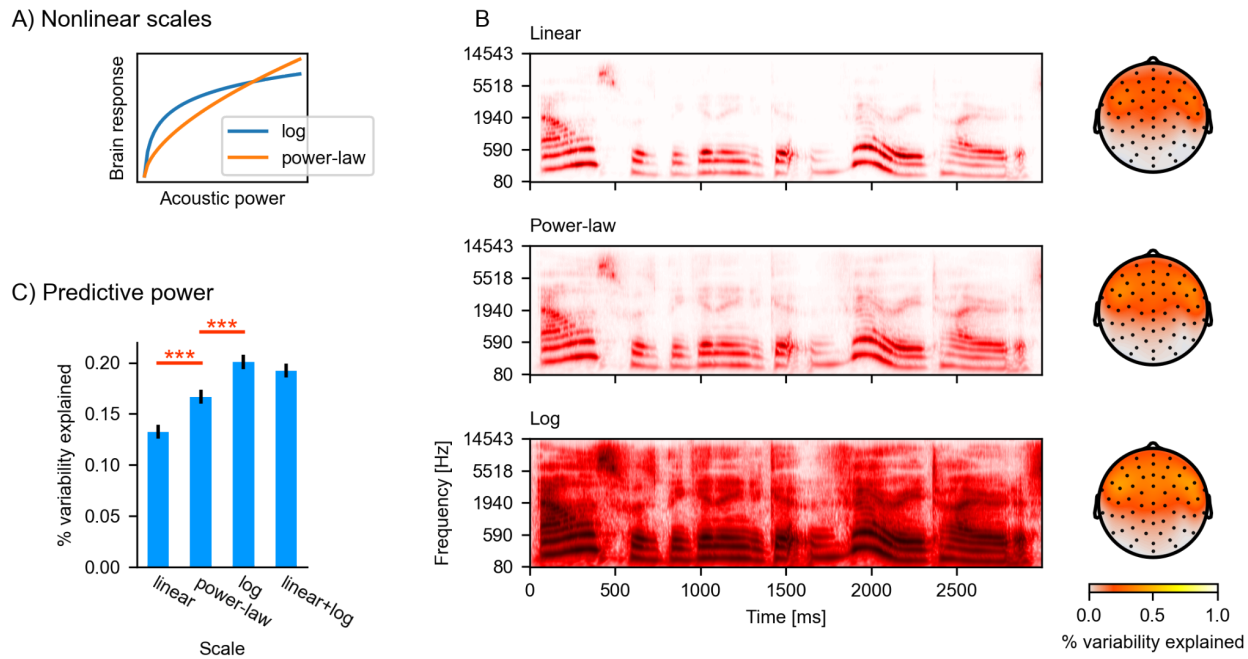

Figure 7. Nonlinear response scales.
(**A**) Illustration of logarithmic and power-law scales. (**B**) Gammatone spectrograms transformed to correspond to linear, power-law and logarithmic response scales. Topographic maps show the predictive power of the three different spectrogram models (the colorbar represents percent of the variability in the EEG data that is explained by the respective mTRF model). (**C**) Statistical comparison of the predictive power, averaged across all sensors.
***: $p \leq .001$; Source code: figures/Auditory-scale.py

Figure 7-B shows the gammatone spectrogram, transformed to linear, power-law and logarithmic response scales, along with the predictive power for EEG data resulting from the different transformations. When considering the average predictive power at all electrodes, the power-law scale spectrogram was a better predictor than linear scale ($t(32) = 4.59$, $p < .001$), and the log scale further improved predictions compared to the power-law scale ($t(32) = 4.67$, $p < .001$). Furthermore, nonlinear responses may mix properties of different scales. We thus tested whether the response may exhibit a linear component in addition to the logarithmic

component by fitting a model including both the linear and the logarithmic spectrogram (i.e., twice as many predictors; similarly, polynomial regression combines multiple nonlinear transformations (Fox, 2008)). The linear+log combined model did not improve predictions over the linear model (Figure 7-C), suggesting that the EEG responses to the acoustic power are sufficiently described by the logarithmic response scale and do not contain an additional linear component.

4.2 Auditory response functions

One goal of perception is to detect complex patterns present in the input signal, and we thus expect brain responses to represent features beyond simple acoustic intensity. Such features can be described as increasingly complex nonlinear transformations. Here we illustrate this using acoustic onsets, a nonlinear transformation that is associated with strong responses and is a critical potential confound for higher level features (Daube et al., 2019). Acoustic features of speech input are shown in Figure 8-A: The upper panel shows the log-transformed gammatone spectrogram, quantifying acoustic energy as a function of time in different frequency bands. The gammatone filters simulate response characteristics of the peripheral auditory system. A simplified, one-dimensional representation of this spectrogram is the envelope, which is the summed energy across all frequency bands (blue line). The lower panel of Figure 8-A shows an acoustic onset spectrogram based on a neurally inspired acoustic edge detection model (Fishbach et al., 2001), as described in Brodbeck et al. (2020). Again, a simplified one-dimensional version of this predictor, summing across all bands, signifies the presence of onsets across frequency bands (blue line).

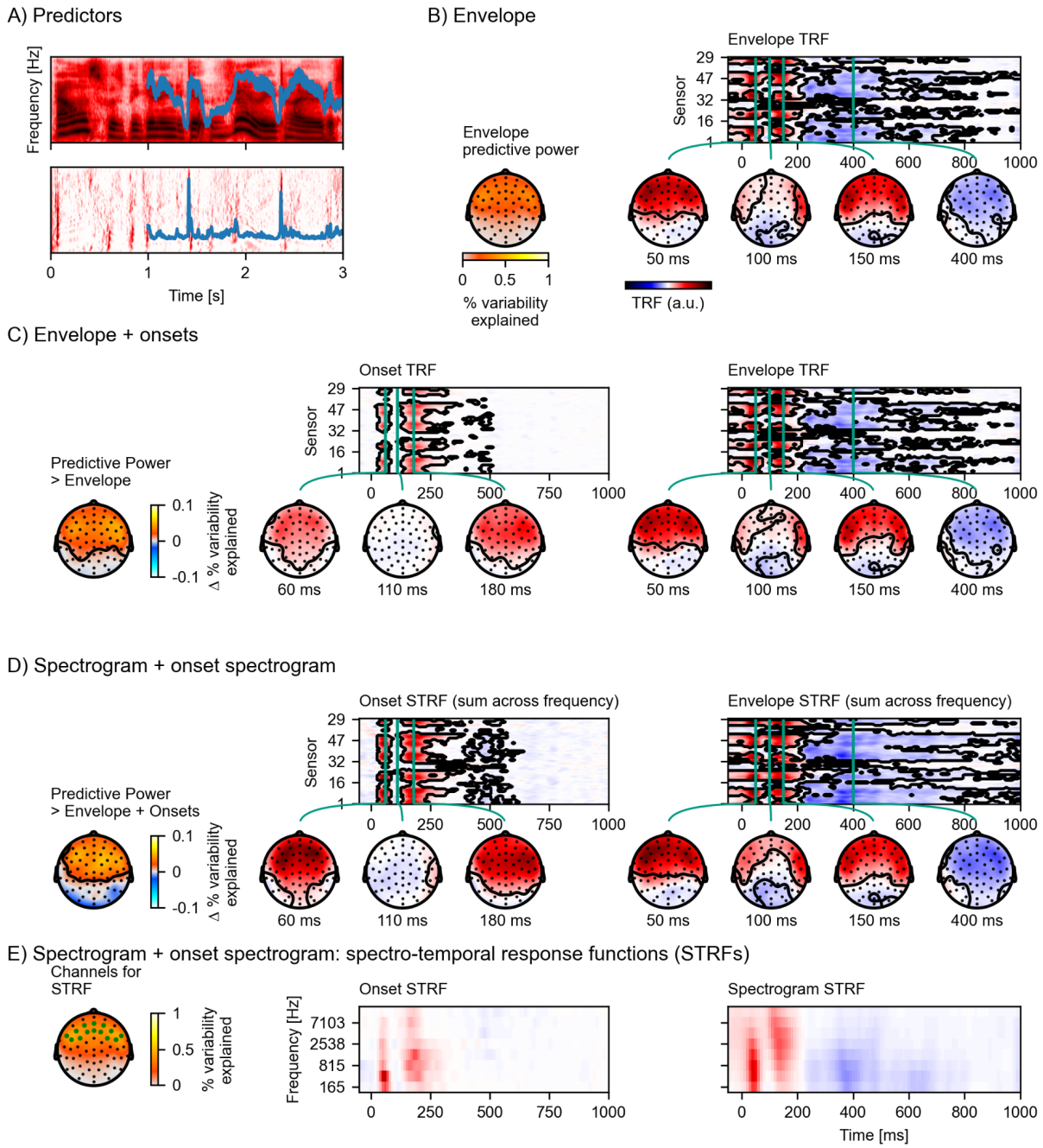
A) Predictors
Frequency [Hz]
Time [s]
B) Envelope
Envelope TRF
Sensor
Envelope predictive power
% variability explained
TRF (a.u.)
50 ms
100 ms
150 ms
400 ms
C) Envelope + onsets
Onset TRF
Envelope TRF
Predictive Power > Envelope
Δ % variability explained
60 ms
110 ms
180 ms
D) Spectrogram + onset spectrogram
Onset STRF (sum across frequency)
Envelope STRF (sum across frequency)
Predictive Power > Envelope + Onsets
E) Spectrogram + onset spectrogram: spectro-temporal response functions (STRFs)
Channels for STRF
% variability explained
Onset STRF
Spectrogram STRF
Frequency [Hz]
Time [ms]

Figure 8. Auditory temporal response functions.
(**A**) Common representations of auditory speech features: an auditory spectrogram (upper panel), and the acoustic envelope, tracking total acoustic energy across frequencies over time (blue line); and an acoustic onset spectrogram (lower panel), also with a one-dimensional summary characterizing the presence of acoustic onsets over time (blue line). (**B**) Brain responses predicted from the acoustic envelope of speech alone. Left: Cross-validated predictive power is highly significant ($p < .001$) at a large cluster covering most anterior sensors. The black outline marks a cluster in which the predictive power is significantly larger than chance ($p \leq .05$, family-wise error correction for the whole head map; colorbar represents percent variability explained). Right: the envelope TRF – the y-axis represents the different EEG channels (in an arbitrary order), and the x-axis represents predictor-response time lags. The green vertical lines indicate specific (manually selected) time points of interest, for which head map topographies are shown. The black outlines mark significant clusters ($p \leq .05$, correction for the whole TRF). For the boosting algorithm, predictors and responses are typically normalized, and the TRF is here analyzed and displayed in this normalized scale. (**C**) Results for an mTRF model including the acoustic envelope and acoustic onsets (blue lines in A). The left-most head map shows the percentage *increase* in predictive power over the TRF model using just the envelope ($p < .001$; colorbar represents change in percent variability explained). Details are analogous to (B). (**D**) Results for an mTRF model including spectrogram and onset spectrogram, further increasing predictive power over the one-dimensional envelope and onset model ($p < .001$; colorbar represents change in percent variability explained). Since the resulting mTRFs distinguish between different frequencies in the stimulus, they are called spectro-temporal response functions (STRFs). In (D), these STRFs are visualized by summing across the different frequency bands. (**E**) To visualize the sensitivity of the STRFs to the different frequency bands, STRFs are instead averaged across sensors sensitive to the acoustic features. The relevant sensors are marked in the head map on the left, which also shows the predictive power of the full spectro-temporal model (colorbar represents percent variability explained). Because boosting generates sparse STRFs, especially when predictors are correlated, as are adjacent frequency bands in a spectrogram, STRFs were smoothed across frequency bands for visualization.
a.u.: arbitrary units. Source code: figures/Auditory-TRFs.py

To illustrate auditory features of increasing complexity we analyzed the following (m)TRF models:

acoustic envelope (4)

acoustic envelope + acoustic onsets (5)

acoustic spectrogram + onset spectrogram (6)

Figure 8-B shows response characteristics to the acoustic envelope alone. A topographic head-map shows the envelope's predictive power. The envelope alone is already a very good predictor of held-out EEG responses, with variability explained reaching 82% of that of the full spectro-temporal model (6) at anterior electrodes. The TRF to the envelope exhibits features

characteristic of auditory evoked responses to simple acoustic stimuli such as tones or isolated syllables, including a P1-N1-P2 sequence.

Figure 8-C shows the result of adding the one-dimensional acoustic onset predictor to the model. Together, onset and envelope significantly improve the prediction of held-out responses compared to just the envelope ($p < .001$), indicating that the onset representation is able to predict some aspects of the EEG responses that the envelope alone cannot. The typical TRF to the onsets is of shorter duration than that to the envelope, and is characterized by two prominent peaks around 60 and 180 ms. The envelope TRF here is not much affected by adding the onset to the model (compare with Figure 8-B).

Figure 8-D shows the additional benefit of representing the envelope and onsets in different frequency bands, i.e., predicting EEG from an auditory spectrogram and an onset spectrogram (here 8 bands were used in each, for a total of 16 predictors). As the predictors are 2-dimensional (frequency × time), the resulting mTRFs are 3-dimensional (frequency × lag × EEG sensor), posing a challenge for visualization on a two-dimensional page. One approach, assuming that response functions are similar across frequency bands, is to sum responses across frequency bands. As shown in Figure 8-D, this indeed results in response functions that look very similar to the one-dimensional versions of the same predictors (Figure 8-C). To visualize how the response functions differ for different frequency bands in the spectrograms, Figure 8-E shows the full spectro-temporal response functions (STRFs), averaged across the electrodes that are most sensitive to the auditory stimulus features.

In sum, while the acoustic envelope is a powerful predictor of EEG responses to speech, additional acoustic features can improve predictions further, suggesting that they characterize neural representations that are not exhaustively described by the envelope. While the increase in prediction accuracy might seem small, more importantly, it allows the critical inference that the different predictors are characterizing separable neural representations. For instance, a significant response to acoustic onsets (after controlling for the envelope/spectrogram) provides evidence for a nonlinear component of the brain response to speech that represents acoustic onsets. Separating the influence of different predictors is also important because different neural representations can have different response characteristics under different situations. For example, acoustic onsets might be especially important in segregating multiple auditory streams (Brodbeck et al., 2020; Fiedler et al., 2019).

4.3 Word onsets as discrete events: Comparing ERPs and TRFs

While speech is continuous, perception is often characterized through discrete events. For example, in speech, words may be perceived as perceptual units. Such events have been analyzed using ERPs, but they can also be incorporated into an mTRF model, by using predictors that contain impulses at relevant time points (see Figure 1). In contrast to an ERP analysis, the mTRF analysis allows controlling for brain responses related to acoustic processing, and overlapping responses to events (words) that are close in time. Here, we directly compare these two analysis approaches.

Word onset TRFs controlling for acoustic processing were estimated using model (7):

acoustic spectrogram + onset spectrogram + all words (7)

These word onset TRFs are shown in Figure 9 alongside the classical ERP. As expected from earlier discussion, the TRF and ERP patterns are similar. The scalp regions where the two estimates of the brain response to words differ significantly are contoured (assessed via related-measures *t*-tests controlling for multiple comparisons). A prominent difference is that the ERP contains stronger activity in the baseline period, and a larger deflection at late lags (starting at 600 ms), with a topography similar to acoustic activity (compare with Figure 8), indicating artifactual leakage from acoustic responses. Additionally, there is a significant difference at around 200 to 450 ms which could be attributed to the temporal spread of the observed P2 peak in the ERPs. Namely, the P2 peak in the TRF is temporally better defined (i.e., sharper) than in the ERPs.

Consistent with expectations, the ERPs overestimate the responses to words. The elevated baseline activity in particular shows that the ERP is more prone to including brain activity that is not strictly a response to the stimulus feature. This is not surprising considering that the ERP is just an average of neural signals before and after word onsets, which includes, besides the responses to the words, neural responses to the acoustic signal, as well as activities that are not time-locked (including overlapping responses to the previous and next word, given that the average interval between word onsets in this stimulus set is only 334 ms). This highlights an advantage of the TRF paradigm over classical ERPs: the TRF enables characterization of only the neural response time-locked to the particular feature of interest, while explicitly controlling for the variances in other lower level features of the stimuli.

A) Comparison of ERP and TRF at single channel

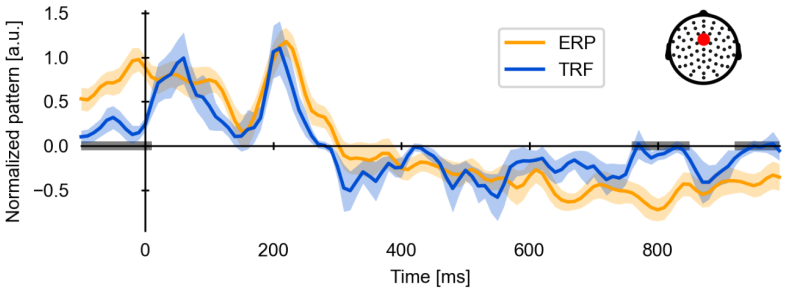

B) Comparison of ERP and TRF across channels

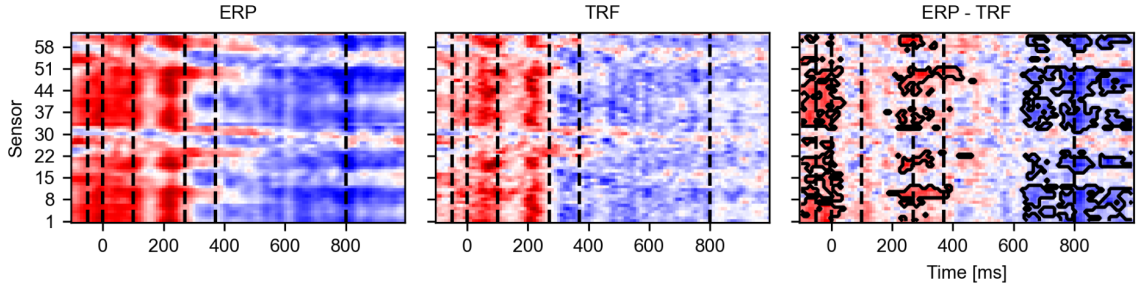

C) Corresponding topographies

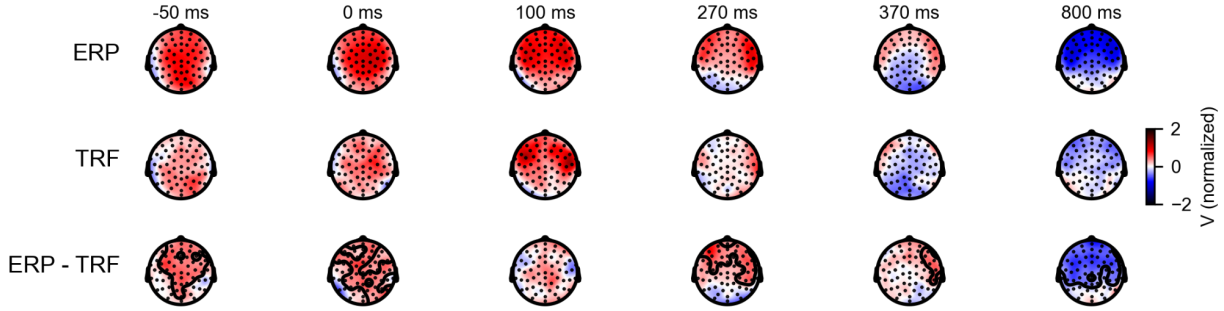

Figure 9. Temporal response functions (TRFs) to discrete events are similar to event-related potentials (ERPs), but control for acoustic processing and overlapping responses.
To visualize ERP and TRF on a similar scale, both ERP and TRF were normalized (parametric normalization). (**A**) Visualization of the ERP and TRF response over time for a frontocentral channel, as indicated on the inset. The gray bars on the time axis indicate the temporal clusters in which the ERP and TRF differ significantly. (**B**) Visualization of ERP and TRF responses across all channels: the ERP responses to word onsets (left), the TRF to word onsets while controlling for acoustic processing (middle), and the difference between the ERP and the TRF (right). The black outline marks clusters in which the ERP and TRF response differs significantly in time and sensors, assessed by a mass-univariate related-measures *t*-test. (**C**) Visualization of the topographies at selected time points, indicated by the vertical, dashed lines in (B), for respectively the ERP (top row), TRF (middle row), and their difference (bottom row). The contours mark regions where the ERP differs significantly from the TRF, as determined by the same mass-univariate related-measures *t*-test as in (B).
a.u.: arbitrary units. Source code: figures/Comparison-ERP-TRF.py

4.4 Categories of events: Function and content words

Given the powerful response to acoustic features of speech, it is important to take these responses into account when investigating linguistic representations. To illustrate the advantage of an mTRF analysis that can take into account the acoustic stimulus features, we revisit an old question: do brain responses differentiate between content words (roughly, words conveying a meaning) and function words (words necessary for a grammatical construction)? In a first, naive approach, we ask literally whether brain responses differ between function and content words, while ignoring any potential confounding influences from acoustic differences. For this, we compare the predictive power of models (8) and (9), all based on predictors with unit magnitude impulses at word onsets:

All words + function words + content words (8)

All words (9)

Note that *all words* and the two word-class-based predictors are mathematically redundant because the *all words* vector equals the sum of the *function words* and *content words* vectors. However, because of the sparsity prior employed through the boosting algorithm and cross-validation, such redundant predictors can still improve a model – for example, if there is a shared response among all words, then attributing this response once as a TRF to *all words* is sparser than attributing it twice, once for *function words* and once for *content words* separately (see also Sparsity prior below).

The predictive power of the model with the word class distinction (8) is significantly higher compared to the model without it (9) at a right anterior electrode cluster (p = .002, Figure 10-A, top). To investigate why the word class distinction improves the model's predictive power, we compare the TRFs to function and content words (Figure 10-B). Both TRFs are reconstructed from the relevant model components: Whenever a function word occurs in the stimulus, there will be both an impulse in the *all words*, and one in the *function words* predictor (and vice versa

for content words). Accordingly, the full EEG response occurring at the function word is split into two components, one in the *all words*, and one in the *function words* TRF. In order to visualize these full EEG responses, the displayed TRF for function words consists of the sum of the TRFs of the *all words* and the *function words* predictors, and the TRF for content words consists of the sum of the TRFs of *all words* and *content words*. This comparison suggests that function words are associated with a larger positive response at anterior sensors than content words.

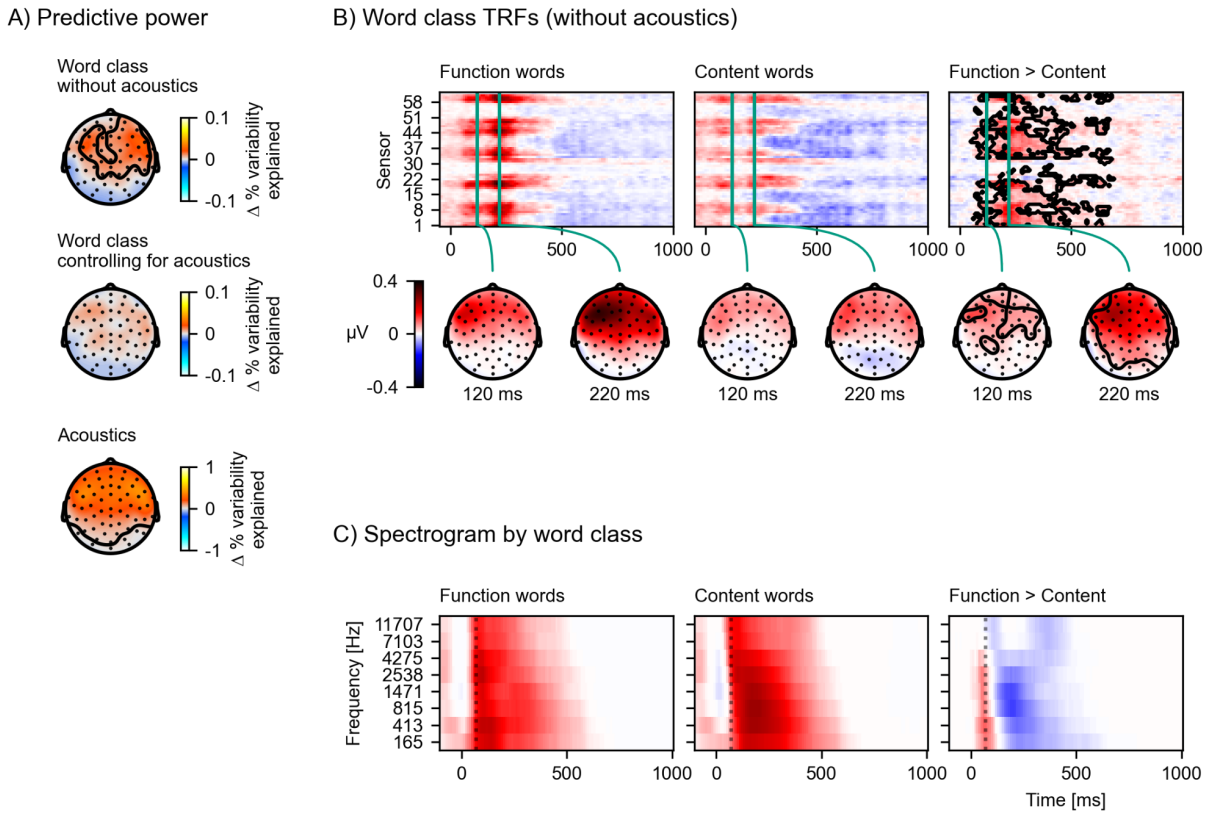

Figure 10. The difference in response to content and function words explained by acoustic differences.
(**A**) Model comparisons of predictive power across the scalp. Each plot shows a head-map of the change in predictive power between different pairs of models. Top: (8) > (9); middle: (10) > (7); bottom: (7) > (9); colorbars represent difference in percent variability explained.. (**B**) Brain responses occurring after function words differ from brain responses after content words. Responses were estimated from the TRFs of model (8) by adding the word-class-specific TRF to the *all words* TRF. The contours mark the regions that are significantly different between function and content words based on a mass-univariate related-measures *t*-test. (**C**) Function words are associated with a sharper acoustic onset than content words. The average spectrograms associated with function and content words were estimated with time-lagged regression, using the same algorithm also used for TRF estimation, but predicting the acoustic spectrogram from the function and content word predictors. A dotted line is plotted at 70 ms to help visual comparison. Color scale is normalized.
Source code: figures/Word-class-acoustic.py

To investigate whether this difference in responses might be due to acoustic confounds, we control for brain responses to acoustic features in both models and compare (10) with (7), repeated here for convenience:

acoustic spectrogram + onset spectrogram + all words + function words + content words (10)

acoustic spectrogram + onset spectrogram + all words (7)

In contrast to the comparison without acoustics, the comparison of the predictive power of (10) with (7) no longer indicates a significant difference (p = .065, Figure 10-A, middle). This suggests that the information in the acoustic predictors can explain the difference between function and content words in model (8). To directly characterize the influence of the acoustic features we plot the predictive power of the acoustic features by comparing models (7) and (9). This comparison suggests that acoustic features are highly predictive of brain signals at anterior sensors (Figure 10-A, bottom), encompassing the region in which the word class distinction originally showed an effect.

If the difference between brain responses to function and content words disappears when controlling for acoustic features, that suggests that acoustic features should differ between function and content words. We can assess this directly with another time-lagged regression model. First, we estimate filter kernels (analogous to the mTRFs) to predict the auditory spectrogram from models (9) and (8) (script: analysis/estimate_word_acoustics.py). To be able to statistically evaluate these results, we use 15-fold cross-validation and treat the predictive accuracy from each test fold as an independent estimate of predictive power (for a similar approach see Etard et al., 2019). With predictive power averaged across frequency bands, the model distinguishing function and content words is significantly better at predicting the spectrogram than the model treating all words equally ($t(14) = 13.49$, $p < .001$), suggesting that function and content words indeed differ acoustically. Finally, the filter kernels to function and

content words from this analysis can be interpreted as average acoustic patterns corresponding to the two word classes (Figure 10-C). This comparison suggests that function words on average have a sharper acoustic onset. Since auditory cortex responses are known to be sensitive to acoustic onsets, a reasonable explanation for the difference in neural responses by word class, when not controlling for acoustic features, is that it reflects these sharper acoustic onsets of function words.

5 Discussion

While the sections above provide recipes for various aspects of mTRF analysis, we use this section to discuss a number of advanced considerations and caveats, and possible extensions.

5.1 TRF analysis vs. predictive power

In the various Results sections, we always tested the predictive power of a predictor variable before analyzing the corresponding TRF. This has good reason: model comparisons based on predictive power are generally more conservative than comparisons based on TRF estimates. First, TRFs are directly estimated on the training data, and are still prone to some overfitting (although the boosting algorithm aims to minimize that using the validation step and early stopping). Second, as in conventional regression models, if two predictors are correlated, that means that they might share some of their predictive power. Model comparisons address this by testing for the *unique* predictive power of a variable, after controlling for all other variables, i.e., by testing for variability in the dependent measure that can *only* be explained by the predictor under investigation. The mTRFs (i.e., regression coefficients) cannot properly be disentangled in this way (Freckleton, 2002), and will usually divide the shared explanatory power amongst themselves. This means that mTRF estimates may always be contaminated by responses to correlated variables, especially when the correlations among predictor variables are high. This consideration highlights the importance of testing predictive power of individual model components before interpreting the corresponding TRFs for avoiding spurious conclusions due to correlated predictors. In sum, a significant result in a model comparison provides strong evidence that a given predictor contributes unique predictive power when compared to the other predictors included in the model. In contrast, a significant effect in a TRF should always be interpreted with care, as it may also reflect the influence of other, correlated variables, even if those are included in the model.

TRF analysis may have an additional utility in diagnosing a special relationship between predictors. Assume that the brain represents a signal, say x_t, and this signal can be decomposed into $x_{1,t}$ and $x_{2,t}$ such that $x_t=x_{1,t}+x_{2,t}$. In a model using the predictors $x_{1,t}$ and $x_{2,t}$, both will contribute significantly. Thus, one might conclude that the brain represents two quantities separately, when in fact it represents only the average of them. However, because $x_t=x_{1,t}+x_{2,t}$, TRFs to $x_{1,t}$ and $x_{2,t}$ in the model including only these two predictors should look identical, thus providing a diagnostic for such a case. If the TRF shapes do not look identical, then that means that the properties in $x_{1,t}$ and $x_{2,t}$ are represented at different latencies, i.e., that they are separable.

5.2 Sparsity prior

In its general formulation, mTRF analysis is a regression problem, albeit a high dimensional one. Such high dimensional analysis methods are almost always marred by overfitting. Presence of a large number of free parameters and correlated predictor variables makes the mTRFs prone to discovering noise patterns that are idiosyncratic to the particular dataset, and which do not generalize well to other datasets. Most regression analysis methods deal with this problem through regularization using a well-informed prior and some form of cross-validation. These regularization schemes vary considerably; some employ an explicitly formulated prior, e.g., the regularization in ridge regression (Crosse et al., 2016b); while others are defined on the algorithmic level, e.g., the early stopping criterion for boosting (see Background: The boosting algorithm). The implicit prior in the boosting algorithm promotes sparsity, i.e., it forces unimportant filter kernel coefficients to exactly 0. It has been shown that for problems with large numbers of correlated predictors, the boosting algorithm might be preferable to other sparsity enforcing algorithms such as LASSO (Hastie et al., 2007).

This sparsity prior has some consequences that might be counterintuitive at first. For example, in regression models it is common to center predictors. This does not affect the explanatory power of individual regressors, because a shift in the mean of one predictor will simply lead to a corresponding shift in the coefficient for the intercept term. In contrast to this, a sparsity prior will favor a model with smaller coefficients. Consequently, an uncentered predictor that can explain responses with a small coefficient in the intercept term will be preferable over a centered predictor that requires a large intercept coefficient.

Another consequence of the same preference for sparser models is that sometimes mathematically redundant predictors can improve the predictive power of a model. An example is that when splitting an impulse predictor into two categories, such as when dividing words into function and content words, the original *all words* predictor does not necessarily become redundant (see Categories of events: Function and content words). This can make model construction more complex, but it can also be informative, for example by showing whether there is a common response component to all words, that can be learned better by including an *all words* predictor, in addition to word-class-specific responses.

5.3 Discrete events and coding

In practice, the assumption of millisecond-precise time-locking to force-aligned features might seem hard to defend. For example, identification of clear word and phoneme boundaries is an artificial imposition, because the actual acoustic-phonetic features blend into each other due to co-articulation. An mTRF analysis only requires time-locking on average to produce some consistent responses. Nevertheless, more precise time estimates enhance the model's ability to isolate the response. In order to model cognitive events more precisely, one might thus want to consider alternative event locations, for example the words' uniqueness points instead of word onsets.

Impulse coding is not the only coding that is available. Impulses are based on the linking hypothesis of a fixed amount of response per impulse. An alternative linking hypothesis

assumes that the brain response is increased for the duration of an event. This could be modeled using a step function instead of impulses. Yet another type of hypothesis might concern a modulation of another predictor. For example, the hypothesis that the magnitude of the neural representation of the speech envelope is modulated by how linguistically informative a given segment is can be implemented by scaling the speech envelope according to each phoneme's linguistic surprisal (Donhauser and Baillet, 2020). A related set of questions concerns whether the same predictor is more or less powerful in different experimental conditions (Sohoglu and Davis, 2020).

5.4 Source localization

EEG data is often analyzed at sensor space. However, because each sensor records a mixture of underlying neural (and artifactual) signals from different sources, sensor space data is inherently noisy. When data is recorded from a dense enough sensor array, neural source localization can be used to estimate a reconstruction of the sources contributing to the mixture signal, and assign the different brain responses to their cortical locations (Nunez and Srinivasan, 2006). Approaches combining source localization with mTRF analysis can differentiate responses related to processing of continuous stimuli anatomically as well as temporally, and thus provide a way to investigate hierarchical models of sensory and cognitive processing involving multiple anatomical regions. In many cases, source localization can also improve the signal-to-noise ratio of a specific response, because it acts as a spatial filter, aggregating information that is relevant for a given brain region across sensors, and suppressing signals whose likely origin is a different location.

A straight-forward extension of the approach described here is to apply a linear inverse solution to the continuous data, and apply mTRF analyses to the virtual current dipoles (Brodbeck et al., 2018b). For this purpose, Eelbrain contains functions that directly convert MNE-Python source estimate objects to `NDVars`. A more advanced approach is the Neuro-Current Response Function technique, which performs mTRF estimation and source localization jointly, in a unified estimation problem. This approach allows an mTRF model at each virtual current dipole, and estimates those mTRFs collectively to optimize prediction of MEG measurements in sensor space (Das et al., 2020).

5.5 Choosing the reference strategy

Since EEG data consists of voltage measurements, but only voltage differences are physically meaningful, the choice of referencing strategy matters. There are several common choices for a voltage reference for EEG data, including the average signal recorded at the mastoid electrodes, the central electrode Cz, and the average across all channels (also called the common average reference). Although the reference has minimal influence on the magnitude of the prediction accuracies averaged across channels or the latencies of the TRF peaks, it does have a substantial impact on the distribution across the EEG channels (Figure 11). This is because, depending on the chosen referencing strategy, the neural sources are projected differently across the scalp.

Therefore, the activity of the neural dipoles of interest might be more (or less) prominent depending on the chosen referencing strategy.

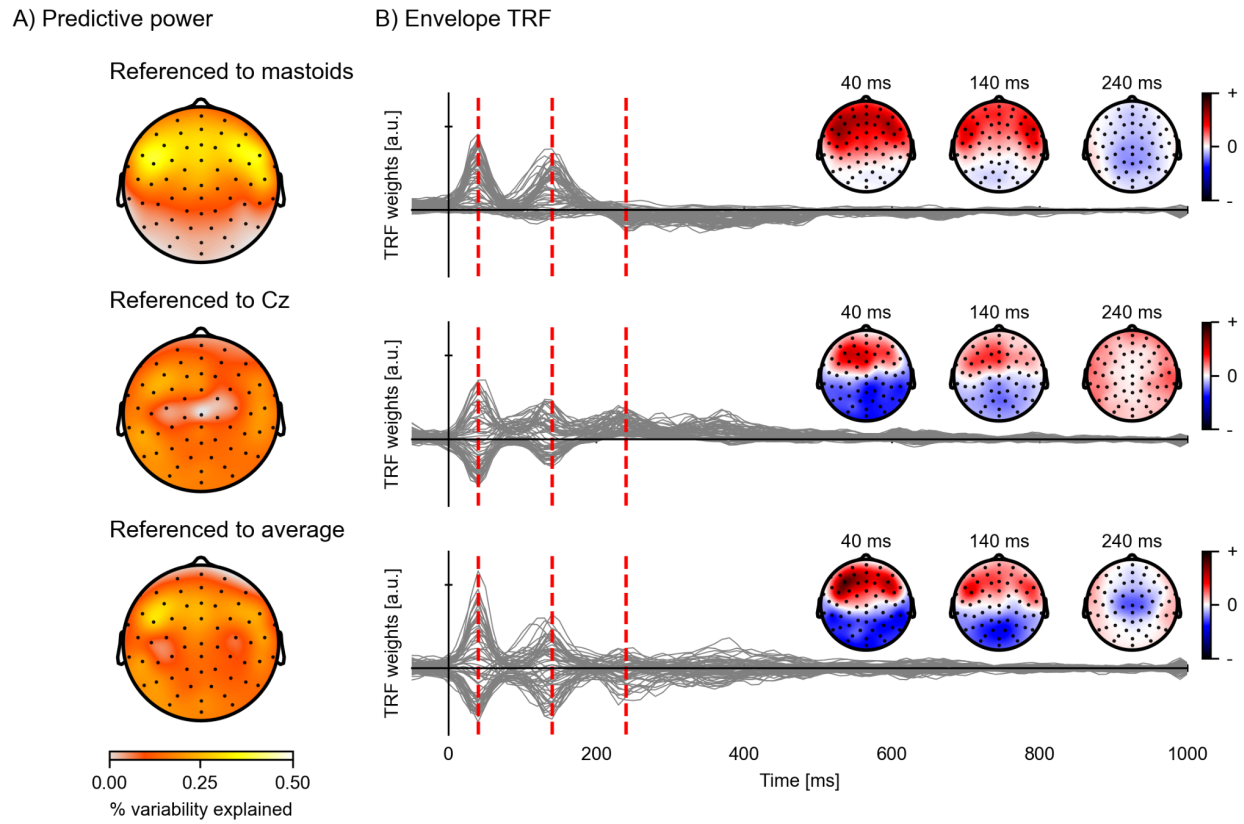

Figure 11. Comparison of EEG reference strategies.
Predictive power topographies and TRFs for an envelope model according to three different referencing strategies: mastoids (top), the central electrode Cz (middle), and the common average (bottom). (**A**) Visualization of the predictive power obtained with the different referencing strategies (colorbar represents percent variability explained). (**B**) The envelope TRFs for the different referencing strategies. The insets indicate the topographies corresponding to the vertical red dashed lines at latencies of 40, 140, and 240 ms.
Source code: figures/Reference-strategy.py

5.6 Further applications

While cortical processing of speech has been a primary application for mTRF analysis, the technique has potential applications in any domain where stimuli unfold in time, and has already been successfully applied to music perception (Di Liberto et al., 2020; Leahy et al., 2021), audiovisual speech perception (Crosse et al., 2016a), and subcortical auditory processing (Maddox and Lee, 2018). Furthermore, mTRF analysis as discussed here assumes that TRFs are static across time. However, this is not always a valid assumption. For example, in multi-talker speech, TRFs to speech features change as a function of whether the listener attends to the given speech stream or not (Ding and Simon, 2012; Brodbeck et al., 2018a; Broderick et al.,

2018). Thus, moment-to-moment fluctuations in attention might be associated with corresponding changes in the TRFs. While modeling this is a highly complex problem, with an even larger number of degrees of freedom, some initial progress has been made towards estimating mTRF models with dynamic TRFs that can change over time (Babadi et al., 2010; Miran et al., 2018; Presacco et al., 2019).

5.7 Conclusions

TRF analysis has several advantages over ERP based methods. In the Results section we demonstrated, with several examples, how TRFs can be used to estimate the brain response associated with a given feature while controlling for (1) responses associated with other features that are correlated with the feature of interest, including correlations across different time lags (e.g., controlling for acoustics while analyzing responses to words), and (2) overlapping responses to events close in time (e.g., disentangling early responses to the current word from late responses to the previous word). In addition, analysis of the prediction accuracy allows determining whether a given feature makes a unique contribution over and beyond other features of the same stimulus. This is especially important in naturalistic stimuli where features are correlated in complex ways, because neural response estimates may be reliably different from zero even if the corresponding predictor does not provide unique predictive power. Finally, using cross-validation, models are assessed based on their *predictive* power, not just their *explanatory* power, thus providing an overall stronger test than conventional models.

6 Acknowledgements

We are grateful for support from the following grants: NSF BCS 1754284, NSF BCS 2043903 & NSF IIS 2207770 (CB); NSF SMA 1734892 (JPK & JZS); NIH R01 DC014085 (JPK & JZS); NIH R01 DC019394 (JZS); FWO SB 1SA0620N (MG); ONR MURI N00014-18-1-2670 (SB & PR); and NIH T32 DC017703 (PG).

7 Data Availability

The data analyzed here was originally released with DOI: 10.7302/Z29C6VNH and can be retrieved from https://deepblue.lib.umich.edu/data/concern/data_sets/bg257f92t. For the purpose of this tutorial, the data were restructured and rereleased with DOI: 10.13016/pulf-lndn at http://hdl.handle.net/1903/27591. Intermediate results (the TRFs) can also be downloaded from that location. The companion GitHub repository contains instructions on replicating the analyses, including a downloader script for the data (https://github.com/Eelbrain/Alice).

8 References

Alday PM. 2019. M/EEG analysis of naturalistic stories: a review from speech to language

processing. *Lang Cogn Neurosci* **34**:457–473. doi:10.1080/23273798.2018.1546882
Babadi B, Kalouptsidis N, Tarokh V. 2010. SPARLS: The Sparse RLS Algorithm. *IEEE Trans Signal Process* **58**:4013–4025. doi:10.1109/TSP.2010.2048103
Bhattasali S, Brennan J, Luh W-M, Franzluebbers B, Hale J. 2020. The Alice Datasets: fMRI & EEG Observations of Natural Language ComprehensionProceedings of the 12th Conference on Language Resources and Evaluation. Presented at the LREC 2020. Marseille. pp. 120–125.
Biesmans W, Das N, Francart T, Bertrand A. 2017. Auditory-Inspired Speech Envelope Extraction Methods for Improved EEG-Based Auditory Attention Detection in a Cocktail Party Scenario. *IEEE Trans Neural Syst Rehabil Eng* **25**:402–412. doi:10.1109/TNSRE.2016.2571900
Brennan JR, Hale JT. 2019. Hierarchical structure guides rapid linguistic predictions during naturalistic listening. *PLOS ONE* **14**:e0207741. doi:10.1371/journal.pone.0207741
Brodbeck C, Bhattasali S, Cruz Heredia AA, Resnik P, Simon JZ, Lau E. 2022. Parallel processing in speech perception with local and global representations of linguistic context. *eLife* **11**:e72056. doi:10.7554/eLife.72056
Brodbeck C, Hong LE, Simon JZ. 2018a. Rapid Transformation from Auditory to Linguistic Representations of Continuous Speech. *Curr Biol* **28**:3976-3983.e5. doi:10.1016/j.cub.2018.10.042
Brodbeck C, Jiao A, Hong LE, Simon JZ. 2020. Neural speech restoration at the cocktail party: Auditory cortex recovers masked speech of both attended and ignored speakers. *PLOS Biol* **18**:e3000883. doi:10.1371/journal.pbio.3000883
Brodbeck C, Presacco A, Simon JZ. 2018b. Neural source dynamics of brain responses to continuous stimuli: Speech processing from acoustics to comprehension. *NeuroImage* **172**:162–174. doi:10.1016/j.neuroimage.2018.01.042
Brodbeck C, Simon JZ. 2020. Continuous speech processing. *Curr Opin Physiol* **18**:25–31. doi:10.1016/j.cophys.2020.07.014
Broderick MP, Anderson AJ, Liberto GMD, Crosse MJ, Lalor EC. 2018. Electrophysiological Correlates of Semantic Dissimilarity Reflect the Comprehension of Natural, Narrative Speech. *Curr Biol* **28**:803-809.e3. doi:10.1016/j.cub.2018.01.080
Crosse MJ, Di Liberto GM, Lalor EC. 2016a. Eye Can Hear Clearly Now: Inverse Effectiveness in Natural Audiovisual Speech Processing Relies on Long-Term Crossmodal Temporal Integration. *J Neurosci* **36**:9888–9895. doi:10.1523/JNEUROSCI.1396-16.2016
Crosse MJ, Liberto D, M G, Bednar A, Lalor EC. 2016b. The Multivariate Temporal Response Function (mTRF) Toolbox: A MATLAB Toolbox for Relating Neural Signals to Continuous Stimuli. *Front Hum Neurosci* **10**. doi:10.3389/fnhum.2016.00604
Crosse MJ, Zuk NJ, Di Liberto GM, Nidiffer AR, Molholm S, Lalor EC. 2021. Linear Modeling of Neurophysiological Responses to Speech and Other Continuous Stimuli: Methodological Considerations for Applied Research. *Front Neurosci* **15**:705621. doi:10.3389/fnins.2021.705621
Das P, Brodbeck C, Simon JZ, Babadi B. 2020. Neuro-current response functions: A unified approach to MEG source analysis under the continuous stimuli paradigm. *NeuroImage* **211**:116528. doi:10.1016/j.neuroimage.2020.116528
Daube C, Ince RAA, Gross J. 2019. Simple Acoustic Features Can Explain Phoneme-Based

Predictions of Cortical Responses to Speech. *Curr Biol* **29**:1924-1937.e9. doi:10.1016/j.cub.2019.04.067
David SV, Mesgarani N, Shamma SA. 2007. Estimating sparse spectro-temporal receptive fields with natural stimuli. *Netw Comput Neural Syst* **18**:191–212. doi:10.1080/09548980701609235
David SV, Shamma SA. 2013. Integration over Multiple Timescales in Primary Auditory Cortex. *J Neurosci* **33**:19154–19166. doi:10.1523/JNEUROSCI.2270-13.2013
Di Liberto GM, Pelofi C, Bianco R, Patel P, Mehta AD, Herrero JL, de Cheveigné A, Shamma S, Mesgarani N. 2020. Cortical encoding of melodic expectations in human temporal cortex. *eLife* **9**:e51784. doi:10.7554/eLife.51784
Di Liberto GM, O'Sullivan JA, Lalor EC. 2015. Low-Frequency Cortical Entrainment to Speech Reflects Phoneme-Level Processing. *Curr Biol* **25**:2457–2465. doi:10.1016/j.cub.2015.08.030
Ding N, Chatterjee M, Simon JZ. 2014. Robust cortical entrainment to the speech envelope relies on the spectro-temporal fine structure. *NeuroImage* **88**:41–46. doi:10.1016/j.neuroimage.2013.10.054
Ding N, Simon JZ. 2012. Emergence of neural encoding of auditory objects while listening to competing speakers. *Proc Natl Acad Sci U S A* **109**:11854–9. doi:10.1073/pnas.1205381109
Donhauser PW, Baillet S. 2020. Two Distinct Neural Timescales for Predictive Speech Processing. *Neuron* **105**:385-393.e9. doi:10.1016/j.neuron.2019.10.019
Etard O, Kegler M, Braiman C, Forte AE, Reichenbach T. 2019. Decoding of selective attention to continuous speech from the human auditory brainstem response. *NeuroImage* **200**:1–11. doi:10.1016/j.neuroimage.2019.06.029
Fiedler L, Wöstmann M, Graversen C, Brandmeyer A, Lunner T, Obleser J. 2017. Single-channel in-ear-EEG detects the focus of auditory attention to concurrent tone streams and mixed speech. *J Neural Eng* **14**:036020. doi:10.1088/1741-2552/aa66dd
Fiedler L, Wöstmann M, Herbst SK, Obleser J. 2019. Late cortical tracking of ignored speech facilitates neural selectivity in acoustically challenging conditions. *NeuroImage* **186**:33–42. doi:10.1016/j.neuroimage.2018.10.057
Fishbach A, Nelken I, Yeshurun Y. 2001. Auditory Edge Detection: A Neural Model for Physiological and Psychoacoustical Responses to Amplitude Transients. *J Neurophysiol* **85**:2303–2323. doi:10.1152/jn.2001.85.6.2303
Fox J. 2008. Applied regression analysis and generalized linear models, 2nd ed. ed. Los Angeles: Sage.
Freckleton RP. 2002. On the misuse of residuals in ecology: regression of residuals vs. multiple regression. *J Anim Ecol* **71**:542–545. doi:10.1046/j.1365-2656.2002.00618.x
Gillis M, Vanthornhout J, Simon JZ, Francart T, Brodbeck C. 2021. Neural markers of speech comprehension: measuring EEG tracking of linguistic speech representations, controlling the speech acoustics. *bioRxiv* 2021.03.24.436758. doi:10.1101/2021.03.24.436758
Gramfort A, Luessi M, Larson E, Engemann DA, Strohmeier D, Brodbeck C, Parkkonen L, Hämäläinen MS. 2014. MNE software for processing MEG and EEG data. *NeuroImage* **86**:446–460. doi:10.1016/j.neuroimage.2013.10.027
Hamilton LS, Huth AG. 2020. The revolution will not be controlled: natural stimuli in speech

neuroscience. *Lang Cogn Neurosci* **35**:573–582. doi:10.1080/23273798.2018.1499946
Harris CR, Millman KJ, van der Walt SJ, Gommers R, Virtanen P, Cournapeau D, Wieser E, Taylor J, Berg S, Smith NJ, Kern R, Picus M, Hoyer S, van Kerkwijk MH, Brett M, Haldane A, del Río JF, Wiebe M, Peterson P, Gérard-Marchant P, Sheppard K, Reddy T, Weckesser W, Abbasi H, Gohlke C, Oliphant TE. 2020. Array programming with NumPy. *Nature* **585**:357–362. doi:10.1038/s41586-020-2649-2
Hastie T, Taylor J, Tibshirani R, Walther G. 2007. Forward stagewise regression and the monotone lasso. *Electron J Stat* **1**:1–29. doi:10.1214/07-EJS004
Heeris J. 2018. Gammatone Filterbank Toolkit.
Kulasingham JP, Brodbeck C, Presacco A, Kuchinsky SE, Anderson S, Simon JZ. 2020. High gamma cortical processing of continuous speech in younger and older listeners. *NeuroImage* **222**:117291. doi:10.1016/j.neuroimage.2020.117291
Kulasingham JP, Simon JZ. 2022. Algorithms for Estimating Time-Locked Neural Response Components in Cortical Processing of Continuous Speech. *IEEE Trans Biomed Eng* 1–9. doi:10.1109/TBME.2022.3185005
Lalor EC, Foxe JJ. 2010. Neural responses to uninterrupted natural speech can be extracted with precise temporal resolution. *Eur J Neurosci* **31**:189–193. doi:10.1111/j.1460-9568.2009.07055.x
Lalor EC, Pearlmutter BA, Reilly RB, McDarby G, Foxe JJ. 2006. The VESPA: A method for the rapid estimation of a visual evoked potential. *NeuroImage* **32**:1549–1561. doi:10.1016/j.neuroimage.2006.05.054
Leahy J, Kim S-G, Wan J, Overath T. 2021. An Analytical Framework of Tonal and Rhythmic Hierarchy in Natural Music Using the Multivariate Temporal Response Function. *Front Neurosci* **0**. doi:10.3389/fnins.2021.665767
Maddox RK, Lee AKC. 2018. Auditory Brainstem Responses to Continuous Natural Speech in Human Listeners. *eneuro* **5**:ENEURO.0441-17.2018. doi:10.1523/ENEURO.0441-17.2018
Maris E, Oostenveld R. 2007. Nonparametric statistical testing of EEG- and MEG-data. *J Neurosci Methods* **164**:177–190. doi:10.1016/j.jneumeth.2007.03.024
McAuliffe M, Socolof M, Mihuc S, Wagner M, Sonderegger M. 2017. Montreal Forced Aligner: Trainable Text-Speech Alignment Using KaldiInterspeech 2017. Presented at the Interspeech 2017. ISCA. pp. 498–502. doi:10.21437/Interspeech.2017-1386
Miran S, Akram S, Sheikhattar A, Simon JZ, Zhang T, Babadi B. 2018. Real-Time Tracking of Selective Auditory Attention From M/EEG: A Bayesian Filtering Approach. *Front Neurosci* **12**. doi:10.3389/fnins.2018.00262
Nichols TE, Holmes AP. 2002. Nonparametric permutation tests for functional neuroimaging: A primer with examples. *Hum Brain Mapp* **15**:1–25. doi:10.1002/hbm.1058
Nunez PL, Srinivasan R. 2006. Electric Fields of the Brain: The Neurophysics of EEG, 2nd ed. Oxford: Oxford University Press.
O'Sullivan JA, Power AJ, Mesgarani N, Rajaram S, Foxe JJ, Shinn-Cunningham BG, Slaney M, Shamma SA, Lalor EC. 2015. Attentional Selection in a Cocktail Party Environment Can Be Decoded from Single-Trial EEG. *Cereb Cortex* **25**:1697–1706. doi:10.1093/cercor/bht355
Patterson RD, Robinson K, Holdsworth J, McKeown D, Zhang C, Allerhand M. 1992. Complex Sounds and Auditory ImagesAuditory Physiology and Perception. Elsevier. pp. 429–446. doi:10.1016/B978-0-08-041847-6.50054-X

Presacco A, Miran S, Babadi B, Simon JZ. 2019. Real-Time Tracking of Magnetoencephalographic Neuromarkers during a Dynamic Attention-Switching Task2019 41st Annual International Conference of the IEEE Engineering in Medicine and Biology Society (EMBC). Presented at the 2019 41st Annual International Conference of the IEEE Engineering in Medicine and Biology Society (EMBC). pp. 4148–4151. doi:10.1109/EMBC.2019.8857953

R Core Team. 2021. R: A Language and Environment for Statistical Computing. Vienna, Austria: R Foundation for Statistical Computing.

Rahman M, Willmore BDB, King AJ, Harper NS. 2020. Simple transformations capture auditory input to cortex. *Proc Natl Acad Sci* **117**:28442–28451. doi:10.1073/pnas.1922033117

Reback J, Jbrockmendel, McKinney W, Van Den Bossche J, Augspurger T, Cloud P, Hawkins S, Gfyoung, Sinhrks, Roeschke M, Klein A, Terji Petersen, Tratner J, She C, Ayd W, Hoefler P, Naveh S, Garcia M, Schendel J, Hayden A, Saxton D, Shadrach R, Gorelli ME, Jancauskas V, Fangchen Li, Attack68, McMaster A, Battiston P, Skipper Seabold, Kaiqi Dong. 2021. Pandas. doi:10.5281/ZENODO.3509134

Salverda AP, Dahan D, McQueen JM. 2003. The role of prosodic boundaries in the resolution of lexical embedding in speech comprehension. *Cognition* **90**:51–89. doi:10.1016/S0010-0277(03)00139-2

Smith SM, Nichols TE. 2009. Threshold-free cluster enhancement: Addressing problems of smoothing, threshold dependence and localisation in cluster inference. *NeuroImage* **44**:83–98. doi:10.1016/j.neuroimage.2008.03.061

Sohoglu E, Davis MH. 2020. Rapid computations of spectrotemporal prediction error support perception of degraded speech. *eLife* **9**:e58077. doi:10.7554/eLife.58077

Theunissen FE, David SV, Singh NC, Hsu A, Vinje WE, Gallant JL. 2001. Estimating spatio-temporal receptive fields of auditory and visual neurons from their responses to natural stimuli. *Netw Comput Neural Syst* **12**:289–316. doi:10.1080/net.12.3.289.316

Vallat R. 2018. Pingouin: statistics in Python. *J Open Source Softw* **3**:1026. doi:10.21105/joss.01026

Weissbart H, Kandylaki KD, Reichenbach T. 2020. Cortical Tracking of Surprisal during Continuous Speech Comprehension. *J Cogn Neurosci* **32**:155–166. doi:10.1162/jocn_a_01467